



Evidences for pre-orogenic passive-margin extension in a Cretaceous fold-and-thrust belt on the basis of combined seismic and field data (western Transdanubian Range, Hungary)

Gábor Héja¹ · Szilvia Kövér¹ · Gábor Csillag¹ · András Németh² · László Fodor^{1,3}

Received: 27 March 2018 / Accepted: 9 July 2018
© Springer-Verlag GmbH Germany, part of Springer Nature 2018

Abstract

Combined sedimentological and structural analysis was carried out in the field and on 2D seismic reflection profiles to recognize pre-orogenic structures in a Cretaceous fold-and-thrust belt. Detailed field observations were made in the Keszthely Hills, Western Hungary, while 2D seismic interpretation was carried out in the neighbouring Zala Basin. As a result, a fault-controlled intraplate basin system was identified by a detailed analysis of bounding faults, and related outcrop-scale structures. The Norian–Rhaetian (227–201.3 Ma) synsedimentary faulting was associated with talus breccia formation, small-scale faulting, and dyke formation, in addition to slumping and other soft-sediment deformations. Based on the distribution of talus breccia, WNW–ESE-trending map-scale normal faults were identified in the Keszthely Hills, which is in agreement with the directly observed outcrop-scale synsedimentary faults. On seismic sections, similar WNW- or NW-trending Late Triassic normal faults were identified based on thickness variations of the syn-rift sediments and the presence of wedge-shaped bodies of talus breccia. Normal faulting occurred already in the Norian, and extensional tectonics was active through the Early and Middle Jurassic. The Late Triassic grabens of the western Transdanubian Range could be correlated with those in western part of the Southern Alps, and the Bajuvaric nappe system of the Northern Calcareous Alps. These grabens were situated on the proximal Adriatic margin, and they represent the first sign of the Alpine Tethys rifting. The locus of extension was laterally migrated westward, towards the distal Adriatic margin during Early and Middle Jurassic.

Keywords Pre-orogenic extension · Synsedimentary deformation · Norian tectonics · Alpine Tethys rifting · Triassic paleogeography

Introduction

Pre-orogenic structures have an increasing role in the structural interpretation of thrust and fold belts (Butler et al. 2006). Several balanced sections show that the

retro-deformed original stratigraphy cannot be considered as a layer-cake and prominent pre-orogenic deformation can be recognized (Perez et al. 2016; Yagupsky et al. 2008; De Vicente et al. 2009). Identification, investigation, and understanding the structural geometry, fault pattern, and deformation style of these pre-orogenic structures have primary importance, since these early structures may have a significant effect on the final geometry of subsequent folding and thrusting.

In many cases, structural inheritance is responsible for the development of backthrusts, young-on-older thrust, and compressional structures non-perpendicular to the shortening, such as oblique or lateral ramps (Bonini et al. 2012; Pace et al. 2014; Ustaszewski and Schmid 2006).

In most cases, pre-orogenic faults develop during the passive-margin evolution, before the onset of shortening. However, normal faults can also be re-activated or newly evolve later, during foreland basin evolution, due to the

Electronic supplementary material The online version of this article (<https://doi.org/10.1007/s00531-018-1637-3>) contains supplementary material, which is available to authorized users.

✉ Gábor Héja
hejagabor@hotmail.com

¹ MTA-ELTE Geological, Geophysical and Space Science Research Group of the Hungarian Academy of Sciences at Eötvös University, Budapest, Hungary

² MOL Hungarian Oil and Gas Plc., Budapest, Hungary

³ MTA-ELTE Volcanology Research Group of the Hungarian Academy of Sciences, Budapest, Hungary

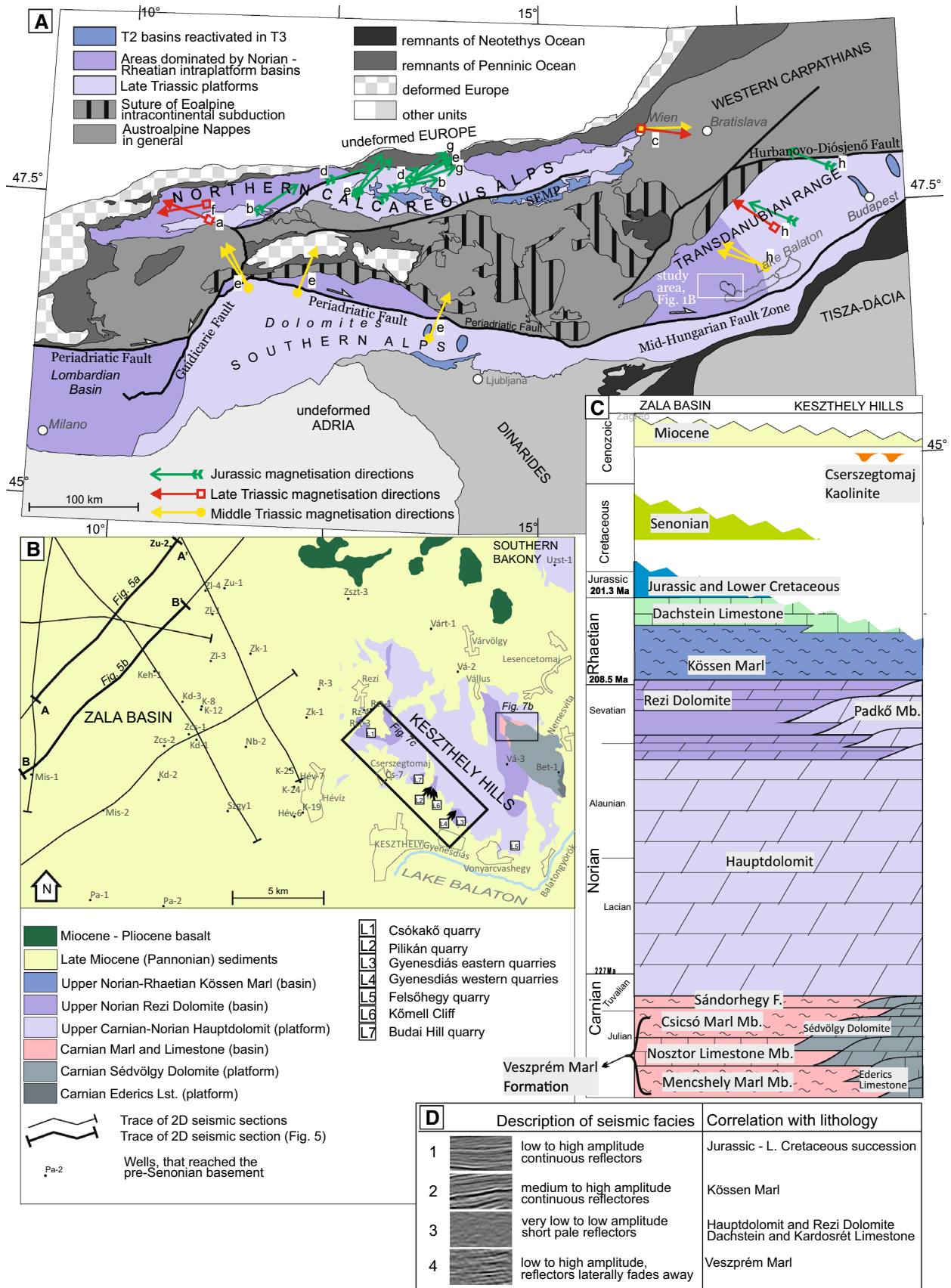


Fig. 1 **a** Position of the study area on the simplified paleogeographic map of the Alps (after Schmid et al. 2008; Goričan et al. 2012; Haas 2002). Austroalpine cover nappes were coloured on the basis of their dominant Late Triassic depositional environment (basin/platform). Yellow arrows show the Middle, Late Triassic, and Jurassic magnetization directions based on the measurements of **a** Becke and Mauritsch (1985), **b** Channell et al. (1990), **c** Gallet et al. (1998), **d** Heer (1982), **e** Mauritsch (1980), **f** Mauritsch and Becke (1987), **g** Mauritsch and Frisch (1978), and **h** Márton and Márton (1983). **b** Geological map of the study area based on Budai et al. (1999b) and Császár and Gyalog (1982). For coordinates of the investigated outcrops, see Table 1. **c** Stratigraphy of the Keszthely Hills and the Zala Basin based on Csillag et al. (1995) and Kőrössi (1988). Formations are shown in approximately proportion to thickness. **d** Seismic facies types of the pre-Senonian basement of the study area

flexure of the subducting lower plate (Butler et al. 2006; Billi and Salvini 2003).

Investigation of pre-orogenic normal faults is often complicated, since such structures can be strongly overprinted by later compressional deformation in thrust belts. However, pre-orogenic synsedimentary structures are often accompanied by secondary features, which may survive the basin inversion. Such features are abrupt facies changes, reflecting significant changes in depositional environments (e.g., deepening) and characteristic sediments and sedimentary structures related to fault activity. However, synsedimentary extension creates facies change only in those cases, if the rate of extension-related subsidence of the hanging wall is significantly larger than the rate of deposition. If the deposition keeps pace with the subsidence of the hanging wall, both the hanging wall and the footwall can have the same environment, and thus, the fault cannot be identified just on the basis of facies changes. In this case, thickness variation of the pre-orogenic succession can be an indicator of synsedimentary normal faulting. The most characteristic fault-related sediments are coarse-grained talus-cone breccias (Ortner et al. 2008); moreover, synsedimentary fault movements are often associated with soft-sediment deformation (Bergerat et al. 2011).

Pre-orogenic extension in the study area was already supposed by Csillag et al. (1995), based on the presence of coarse breccias and facies distribution. However, they neither determined the exact position of faults nor characterized the fault pattern or the stress field. In our study, we demonstrate how the combined sedimentological and structural observations, fault-slip analysis, geological map interpretations, and 2D seismic sections can be used to identify and characterize pre-orogenic structures in a poorly outcropping area. The study area is the westernmost outcropping part of the Transdanubian Range (Keszthely Hills) and its western continuation submerged below the Cenozoic cover of the Zala basin (Fig. 1a, b). The aim of this paper is to describe the Late Triassic extensional structures, hitherto frequently cited but very rarely characterized. Our results

can contribute to understanding the early phase of passive-margin evolution of the study area.

Geological setting

The Transdanubian Range was part of the Adriatic plate, which was situated between the Neotethys and the Alpine Tethys (Mandl 2000; Csontos and Vörös 2004; Schmid et al. 2008). First phase of rifting during Anisian was related to the opening of the western branch of the Neotethys (Haas et al. 1995; Budai and Vörös 2006), while rifting of the Alpine Tethys initiated during Late Triassic and Early Jurassic (Bertotti et al. 1993; Decarlis et al. 2017).

The following deformations of the Transdanubian Range are related to the closure of these oceans. The partial closure of the western part of the Neotethys led to the folding in the study area during the Albian–Coniacian (Fodor et al. 2017). These structures are discordantly covered by the Senonian strata, and they represent one of the most significant deformations of the Transdanubian Range.

After the final subduction of Alpine Tethys, collision and continental subduction of European plate below Adria occurred during the Late Paleogene. This event led to the eastward extrusion of ALCAPA unit along the Periadriatic Fault (Schmid et al. 2008) (Fig. 1a). The eastern continuation of this structure is the Mid-Hungarian shear-zone, which is located directly south of study area (Balla 1984; Csontos and Nagymarosy 1998; Fodor et al. 1999).

The Pannonian back-arc basin system was formed during the Miocene, in the hinterland of this subduction (Tari 1994; Horváth et al. 2015; Balázs et al. 2016). Therefore, the study area was affected by strong extension, and thus, the studied Keszthely Hills are parts of a Miocene extensional horst bounded by normal faults and grabens, such as the Zala Basin (Fodor et al. 2013).

As it was briefly summarized above, the geodynamic evolution of the study area was affected by the opening and closure of two distinct oceanic systems, and accordingly, it has a complex stratigraphy. In this paper, we focus on the Late Triassic and Jurassic synsedimentary deformations, and therefore, we describe only the coeval sediments in detail.

Late Triassic-to-Early Cretaceous stratigraphy

The oldest known formation of the study area is Carnian in age (Haas et al. 2014). The Carnian basinal marl and limestone (Veszprém Marl and Sándorhegy F.) are laterally interfingering with the coeval carbonate platform (Ederics Formation) (Csillag et al. 1995), which was partly dolomitized (Sédvölgy Dolomite) (Haas et al. 2014).

From the end of the Carnian, the Hauptdolomit Formation was deposited (Fig. 1c). The formation is built up by

Table 1 Location of the investigated outcrops

Name of the outcrop	Latitude	Longitude
1. Csókakő quarry	46.82219	17.23101
2. Pílikán quarry	46.79337	17.27255
3. Gyenesdiás eastern quarry	46.7790	17.29165
4. Gyenesdiás western quarry	46.77971	17.28958
5. Felsőhegy quarry	46.76542	17.33641
6. Kőmell Cliff	46.7842	17.28789
7. Budai Hill quarry	46.8033	17.26448

Projection datum is WGS84

134 thin-layered bituminous dolomite in the study area. Occa-
135 sionally, stromatolite intercalations occur. The formation
136 was deposited in ultra-back-reef–lagoon environment (Fruth
137 and Scherreiks 1984).

138 From the end of Middle Norian (Budai and Kovács 1986),
139 extension-related intraplatform basins were formed, which
140 were filled up by late Middle–Upper Norian Rezi Dolomite
141 and Rhaetian Kössen Marl (Haas 1993; Csillag et al. 1995;
142 Budai and Koloszá 1987; Budai et al. 1999a). Budai and
143 Koloszá (1987) subdivided the Rezi Formation into three
144 members. The lower member is represented by dark-grey
145 cherty bituminous-laminated dolomite. The middle member
146 is made up by the alternation thin-layered and thick-layered
147 dolomite, which often contains re-deposited green algae
148 fragments (Fig. 1c). This middle member was interpreted
149 as a platform progradation tongue of the coeval platform.
150 The upper member is similar to the lower member. Another
151 dolomite breccia lithofacies of the Rezi Dolomit with re-
152 deposited platform-originated blocks were identified in the
153 Csókakő quarry (L1) (Csillag et al. 1995).

154 According to Csillag et al. (1995), the Rezi Dolomite was
155 deposited in a synsedimentary half-graben in the Keszthely
156 Hills. The dolomite breccia represents the fault-bounded
157 talus breccia of a synsedimentary normal fault. On the
158 tectonically controlled elevated areas, carbonate platform
159 environment still persisted. These areas are represented by
160 the footwall of major normal fault bordering the Rezi half-
161 graben, and the opposite edge of the half-graben (Csillag
162 et al. 1995). From the edge of the half-graben, the propaga-
163 tion of platform occurred. Nevertheless, this model does not
164 specify the exact geometry of the basin and the controlling
165 normal faults.

166 The Rhaetian Kössen Marl Formation (Fig. 1c) is poorly
167 exposed; therefore, it is rather known from wells (Haas
168 1993). It is made up by dark-grey-to-black shales with high
169 organic matter content. Thin-bedded limestone intercalations
170 occur frequently within the shale; it is strongly folded due to
171 slumping (Budai and Koloszá 1987).

172 The younger Mesozoic formations were eroded in the
173 Keszthely Hills, partly, due to the mid-Cretaceous folding

(Fig. 1c). However, in the western subsurface continuation
of the Keszthely Hills (eastern Zala Basin) and in the South-
ern Bakony (NE to Keszthely Hills), the younger members
of the pre-Senonian succession could be traced. The Kössen
Marl is interfingering with the limestone of the coeval Rhae-
tian Dachstein platform towards NE, based on well data;
consequently, the Kössen Marl pinches out NE-ward (Haas
1993, 2002). Platform progradation of the few 100 m-thick
Dachstein Formation can also be observed above the Kössen
Marl in several wells of the Zala Basin (Kőrössi 1988).

The carbonate platform environment still existed in ear-
liest Jurassic (Kardosrét Fm.); however, it drowned in the
beginning of Sinemurian, due to extension-related strong
subsidence (Fig. 1c). This extension also created horsts and
grabens (Vörös and Galács 1998). There was hiatus, or just
condensed sedimentation on the top of the submarine horsts,
while thin, pelagic formations deposited with variable lithol-
ogy in the grabens (Haas et al. 1984).

The Lower Jurassic succession is characterized by pelagic
red nodular limestone and grey cherty limestone (Haas et al.
1984; Vörös and Galács 1998). During the Middle Juras-
sic, cherty limestone and radiolarites were deposited. The
Upper Jurassic formations seal both the pre-existing horsts
and the grabens (Vörös and Galács 1998; Haas et al. 1984).

This Upper Jurassic succession is made up by red nodular
limestone and white pelagic cherty limestone. The deposi-
tion of the latter formation is lasted till the Early Cretaceous.
From the Barremian to the Aptian silty sandy pelagic marl,
and then shallow marine limestone were deposited (Haas
et al. 1984).

Methods

In the eastern part of the study area (Keszthely Hills),
Triassic rocks are exposed; their microtectonic and basic
carbonate sedimentologic field observations were carried
out in dolomite quarries. To help the readers, the quarries
were marked by numbers (see after the names of quarries in
Sect. 4, and on map Fig. 1b). The measured structural data
were illustrated on stereoplots. In the adjacent Zala Basin,
Mesozoic basement is under thick Cenozoic cover. There,
the investigation of Mesozoic basement is possible based
on seismic data.

Stereoplots

Several types of structural data were measured in outcrops
of the Keszthely Hills, which were plotted by the software
of Angelier (1990) (for legend, see Fig. 2d). Fault-slip
data rarely contained slicken lines, in most cases, just the
fault planes were measurable. Therefore, fault-slip inver-
sion was not carried out, since at least four slicken line

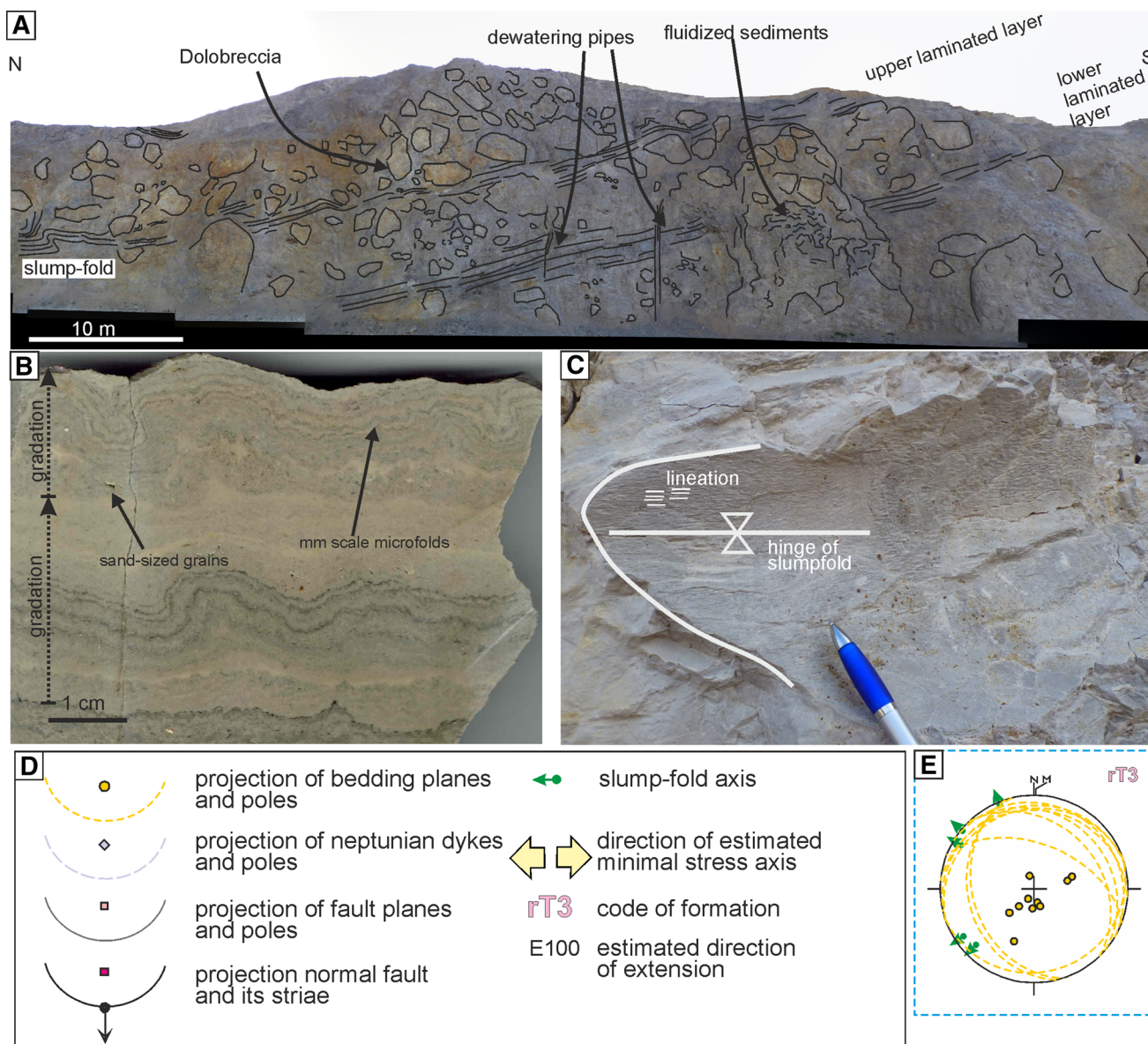


Fig. 2 Eastern wall of the Csókakő quarry (L1). **a** Dolomitic breccia and two laminated dolomite intercalations. Fluidized zones cross cut the dolomite breccia and layers; **b** cm-scale slump folds with mm-

scale microfolds; **c** lineation is visible parallel to the slump-fold axis; **d** legend for the stereonets; **e** stereonet of the measured slump-fold axes and bedding

222 required for the calculation (Angelier 1990). Stress axes
 223 were estimated based on conjugate faults. Tilt test was
 224 carried out by the module of “Rotilt” (Angelier 1990), if
 225 the beds had a significant dip. The basic assumption was
 226 that tilting of the strata is mostly the result of Cretaceous
 227 folding. Pre-orogenic structures were back-tilted by the
 228 dip of the beds, to get a better view on the original geom-
 229 etry. Consequently, tilt test gave a relative chronology with
 230 respect to tilting/folding.

Seismic sections

231

The seismic sections were acquired and processed by GES
 Geophysical Services Ltd. in 2001 using vibroseis source
 with 8–90 Hz sweep frequency. Coverage of 100 and 12.5 m
 distance between CDPs ensured the proper lateral resolution
 and a good signal/noise ratio. These acquisition parameters
 represented an advanced technology that time. This facilitat-
 ed a good image of basement structures. The processing

232
 233
 234
 235
 236
 237
 238

239 was standard time processing including a challenging static
240 correction due to hilly terrain, DMO correction, and post-
241 stack migration. The featured sections were not time-depth
242 converted and the vertical scales show two ways which travel
243 time is second.

244 Field observations

245 Csókakő quarry (L1 on Fig. 1b)

246 Upper Norian Rezi Dolomite is exposed in the Csókakő
247 quarry (L1 on Fig. 1b), which is covered by Upper Miocene
248 (Pannonian) conglomerate and sand. The most spectacular
249 part of the quarry is its eastern wall (Fig. 2a). Two main
250 facies types of the Rezi Dolomite are visible here: thin-lay-
251 ered–laminated dolomite and dolomite breccia. Laminated
252 dolomite occurs in the northern part of the eastern wall with
253 sub-horizontal dip. Southward-thickening dolomite breccia
254 tongues can be observed between the laminated dolomite
255 layers, further south. These strata dip already moderately
256 toward NNE. Further south, the laminated dolomite inter-
257 calations pinch out, and in the southern edge of the quarry,
258 only massive dolomite breccia is present.

259 The laminated unit is characterized by dark grey, strongly
260 bituminous dolomite (Fig. 2a, b, c). Occasionally, sand-sized
261 dolomite lithoclasts can be observed at the base of the lami-
262 nated dolomite layers (Fig. 2b). These layers show normal
263 gradation (Fig. 2b). Slide and slumps are common in the
264 laminated dolomite: slumps occur mostly in the northern
265 part, while slide scarps are more common in the middle
266 and southern parts of the eastern wall. Slump folds shows
267 symmetric to slightly asymmetric geometry; the axes of
268 the slump folds show a significant dispersion, neverthe-
269 less, WNW trend is most frequent (Fig. 2e). Lineation was
270 observed on the slump folds, which is parallel to the fold
271 axis (Fig. 2b, c).

272 The clasts of the dolomite breccia are up to few meters in
273 size (Fig. 2a). They are thick-bedded, white- or light-grey
274 boulders, which often contain green algae, molluscs, and
275 gastropods. Stromatolitic, intertidal dolomite represents
276 another clast type of this dolomite breccia.

277 The matrix of the dolomite breccia is gradually chang-
278 ing south ward. In the northern, distal part of the breccia
279 tongues, the matrix of this dolomite breccia is laminated
280 dolomite. The laminated dolomite matrix is intensively
281 deformed into chaotic folds between the re-deposited large
282 dolomite blocks. In contrast of that, in the southern part
283 of the breccia tongues, the matrix is made up by massive,
284 light-grey dolomite, containing the same platform-originated
285 fossils as the fossil-rich clasts of the dolomite breccia.

286 Two laminated dolomite intercalations are visible
287 between the dolomite breccia tongues in the middle part of

the eastern wall (Fig. 2a). The gently NNE-dipping beds are
cross cut by several, few centimetre wide zones (Fig. 2a).
The infill of these zones is small dolomite breccia clasts
sitting in dolomite matrix.

The lower laminated dolomite layer is interrupted by a
5–10 m-wide sub-vertical collapsed zone, where chaotic,
dark-grey dolomite is mixed with huge, light-grey dolomite
blocks (Fig. 2a). The dark-grey dolomite probably originally
represented the same material as the laminated one, but
its original sedimentary features were destroyed (strongly
deformed) later; therefore, the original lamination cannot
be recognized there (Fig. 2a). The upper laminated dolomite
intercalation is down bending and thickened above this zone
(Fig. 2a).

Very similar, up to meter-sized dolomite blocks were
observed in massive dolomite matrix at the Kőmell Cliff
(L6 on Fig. 1b). Poor outcrop conditions does not permit
detailed description (Fig. 1b).

288 Pilikán quarry (L2 on Fig. 1b)

289 Thinly bedded to laminated, dark-grey, bituminous dolo-
290omite (Rezi Fm.) crops out in the Pilikán quarry (L2). In
291 the southeastern corner of the quarry, a 3 m-thick dolomite
292 breccia intercalation was observed (Fig. 3a). The clasts are
293 significantly smaller than those of the previous outcrops;
294 their maximum size is just few dm (Fig. 3b). The contact of
295 the breccia bed and the underlying dolomite is a wavy ero-
296 sional surface. It is dissected by a number of normal faults
297 (Fig. 3a). The offset of these faults decreasing upward, and
298 finally, they are sealed by cover beds, without any flexure.
299 In the upper part of the eastern wall meter-sized symmetric
300 slump folds occur (Fig. 3a). The thickness variations along
301 the limbs of the slump folds can be observed.

302 On the southern wall, small faults dissect a dark-grey
303 marker bed, with a few cm offset; the overlying layers seal
304 these structures (Fig. 3c). The NW–SE-trending faults show
305 mostly normal offset; however, some of the faults are steep
306 reverse faults (Fig. 3c, d).

307 Similar coarse-grained breccia and symmetric slump
308 folds were observed in the southern Buda Hill quarry (L6
309 on Fig. 1b).

310 Gyenesdiás, eastern quarry (L4 on Fig. 1b)

311 ENE ward dipping beds are dominant in this dolomite
312 quarry; therefore, a relatively thick-tilted succession is vis-
313 ible. In the western wall of the quarry thick beds of Hauptdolo-
314 mit occur, whereas the southern wall exposes the Rezi
315 Dolomite (Fig. 4a). The latter is thin-bedded, laminated,
316 dark-grey bituminous dolomite, in which gentle NW–SE-
317 trending symmetric slump folds were observed. Thick-bed-
318 ded, light-grey dolomite intercalations occur upward, and
319
320
321
322
323
324
325
326
327
328
329
330
331
332
333
334
335
336

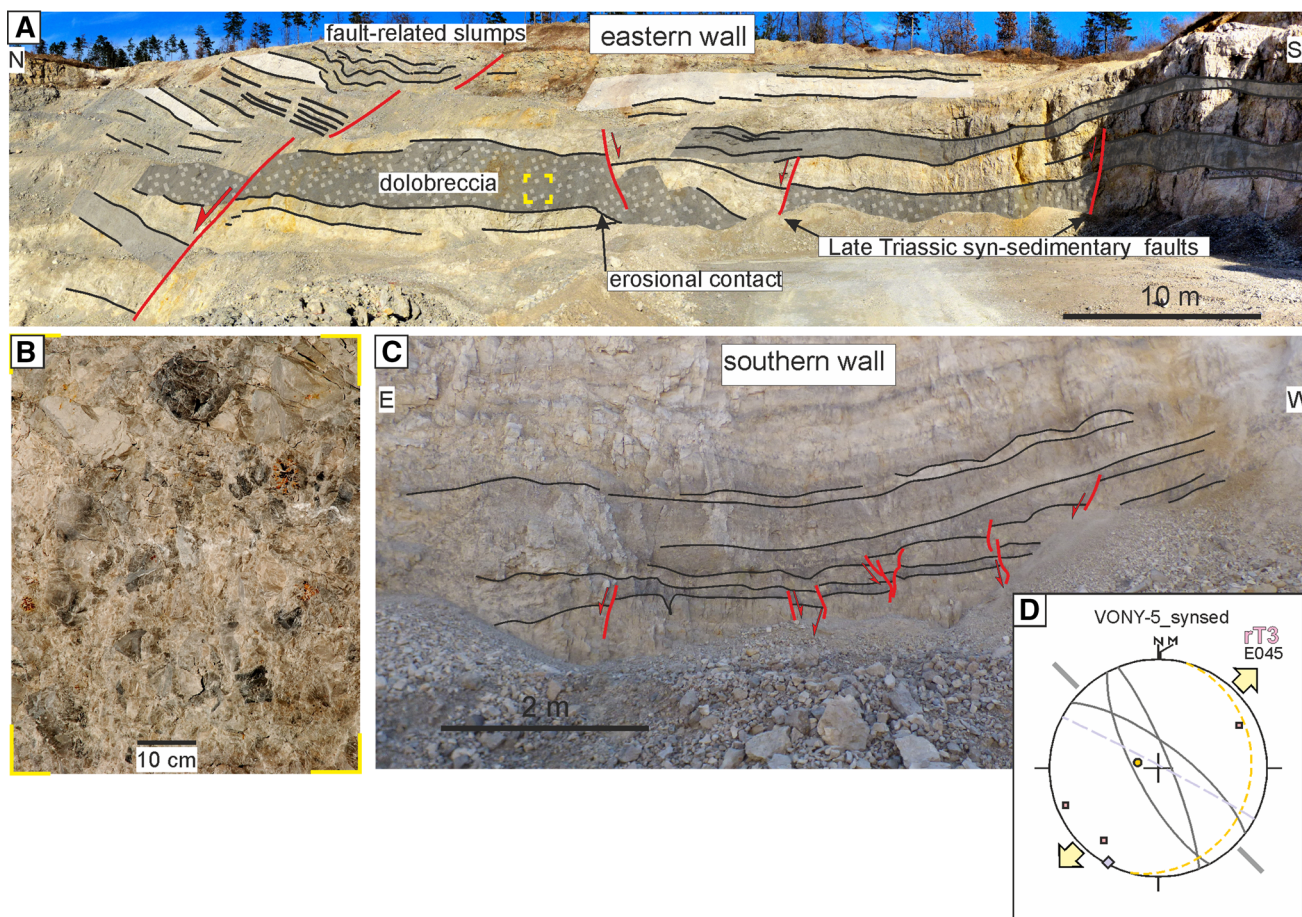


Fig. 3 Pilikán quarry (L2). **a** Dolobreccia intercalation of the Upper Norian Rezi F. on the eastern wall; **b** closer view on dolobreccia; **c** late Triassic synsedimentary faults on the southern wall of the quarry. For legend of the stereonet, see Fig. 2d

337 they dominate the eastern part of the southern wall, whereas,
 338 along the easternmost side, laminated dolomite is present,
 339 again. On the southern wall tilted, conjugate normal fault
 340 pairs were identified (Fig. 4a). The faults have only a few
 341 meter offsets. Back-tilted stereonet suggests NE–SW extension
 342 (Fig. 4.b, c).

343 **Gyenesdiás, western quarry (L3 on Fig. 1b)**

344 This outcrop is situated in the western vicinity of the pre-
 345 viously described quarry (Fig. 1b). It is built up by thin-
 346 bedded, laminated dark-grey Rezi Dolomite. Meso-scale
 347 synsedimentary normal fault/slide was identified with a few
 348 tens of cm offset (Fig. 4d). The beds are thicker in the hang-
 349 ing wall, and the displacement decreases upwards. There
 350 is an upward smoothing extensional fault-related fold/flex-
 351 ure above the fault. It is dissected by minor normal faults
 352 (Fig. 4e). The discrete fault planes of these small-scale str-
 353 uctures are not visible and only the small steps on the bedding
 354 planes indicate them. The faults suggest WNW–ESE exten-
 355 sion (Fig. 4f).

Felső-hegy quarry (L5 on Fig. 1b)

356

This quarry exposes the Hauptdolomit Fm. (Fig. 1b). Thick-
 bedded, light-grey dolomite is the most common, but occa-
 sionally, a few cm thick, black, bituminous dolomite inter-
 beds also occur locally. They contain small, angular clasts
 of light-grey dolomite. The succession is tilted to the NNE.
 On the western wall pre-tilt normal faults were observed
 (Fig. 4g). A dissected, bituminous, dark-grey interlayer has
 increased thickness in the hanging wall. A neptunian dyke
 running parallel to the fault is present in the footwall. It is
 filled by dark-grey, bituminous dolomite. These structures
 suggest NE–SW extension (Fig. 4h).

357
358
359
360
361
362
363
364
365
366
367

Seismic section in the western foreland of the Keszthely Hills

368
369

Two NE–SW-trending segments of 2D seismic sections are
 presented in this paper (Fig. 5a, b), which is situated in the
 northwestern foreland of the Keszthely Hills (Fig. 1b). The

370
371
372

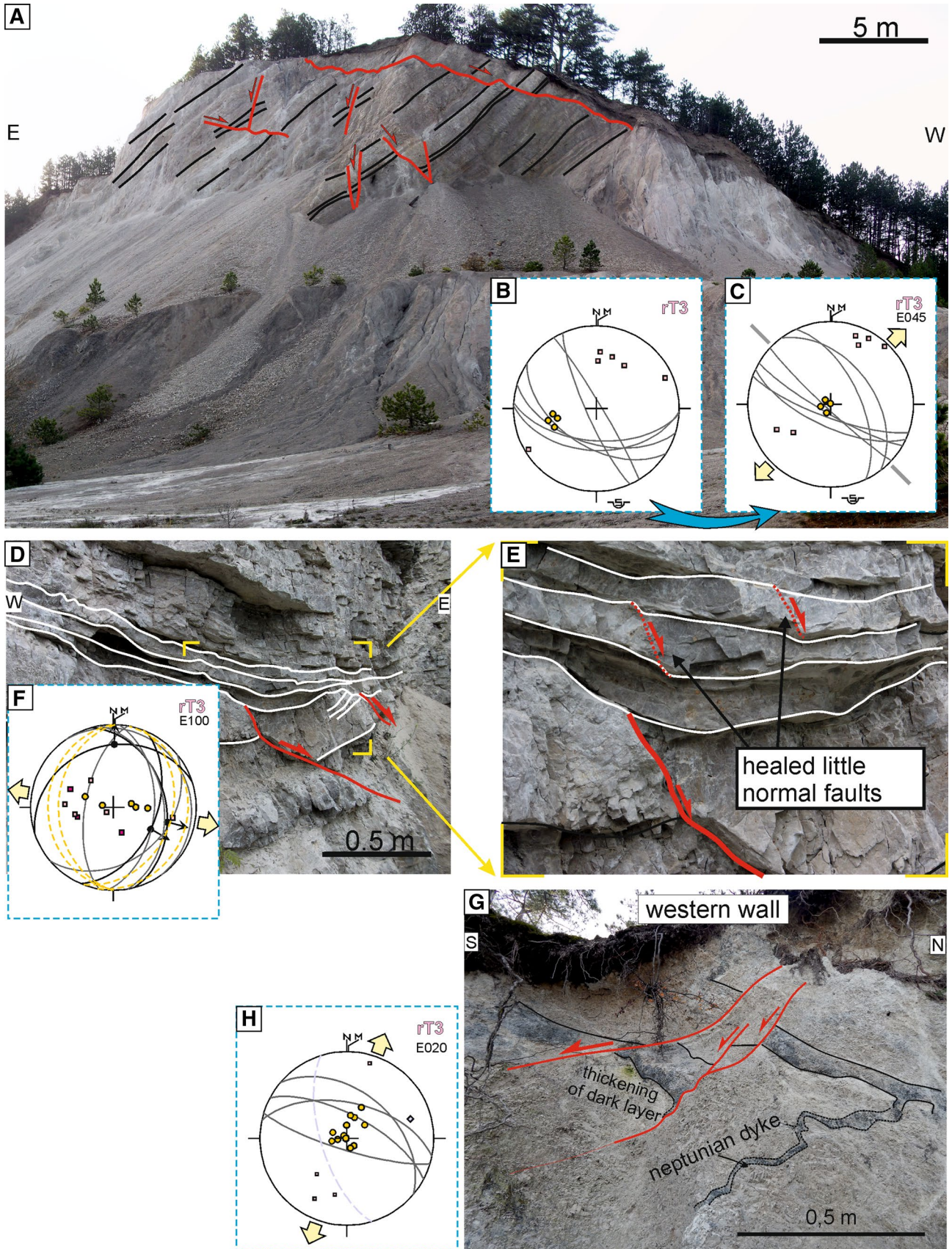


Fig. 4 **a** Tilted normal faults in the eastern Gyenesdiás quarry (L3), observed in Rezi Dolomite. **b** Stereonet data before tilt test. **c** Stereonet of data after tilt test. **d** Gyenesdiás, western quarry (L4). Late Triassic synsedimentary normal fault or slide in the laminated to thin-layered Rezi Dolomite. **f** Measured fault-slip data **g** Late Triassic synsedimentary structures in the Felsőhegy quarry (L5), observed in Hauptdolomit. **h** Measured fault-slip data. Legend for stereonet: Fig. 2d

373 sections run parallel to each other, and they add important
374 new information to the pre-orogenic structures.

375 Seismic facies of the formations

AQ5 The pre-Senonian basement is represented by characteristic
377 features (Figs. 1d, 5a, b). The relatively strong reflection
378 package between 1.6 and 2.2 s TWT depth is equivalent to
379 the Carnian Veszprém Marl. It is characterized by low-to-
380 high amplitude; reflectors laterally often fade away (Fig. 1d),
381 which may represent interfingering with coeval platforms
382 (Ederics Fm.). Veszprém Marl was drilled by the nearby
383 Kd-3 well under 3.4 km of Upper Triassic dolomite. Above
384 this formation, a significantly thick unit without any strong
385 reflections occurs, which is interpreted as the Hauptdolomit
386 and the Rezi Dolomite, which are considered as one seismic
387 unit in this paper. This seismic unit is represented by very
388 low-to-low amplitudes; occasionally, short, pale reflectors
389 occur (Fig. 1d). The thickness of these two dolomite for-
390 mations is around 1 s in time, which suggests more than
391 3 km thickness, applying the VSP data of Dohr (1981). The
392 strong continuous reflections above this unit represent the
393 Kössen Marl. The medium-to-high amplitudes are related
394 to the significant impedance contrast between the marl and
395 the limestone intercalations (Fig. 1d). However, the strong
396 reflections first fade away and then disappear approaching
397 the faults. The thin, non-reflective unit above the Kössen
398 Marl may be correlated to the Upper Rhaetian prograding
399 tongue of the Dachstein and Kardosrét Fm. Consequently,
400 the strong reflections of the Kössen Marl are sandwiched
401 between two, relatively monotonous platform carbonates
402 without reflections. The Jurassic–Early Cretaceous suc-
403 cession, which is made up by thin formations with variable
404 lithologies, shows again relatively strong continuous reflec-
405 tors on seismic sections, which can be characterized by low-
406 to-high amplitude (Figs. 1d, 5a, b).

This Upper Triassic–Lower Cretaceous succession
407 is unconformably overlain by Senonian shallow marine
408 marl with limestone intercalations and platform limestone
409 (Fig. 5a, b). The variable lithology of the Senonian marl
410 causes again continuous reflectors with high amplitude
411 (Fig. 5a), while the relatively monotonous platform lime-
412 stone shows low-amplitude reflectors. On the section A–A',
413 the reflections of the Senonian marl onlap onto the basal
414 surface of the Senonian (Fig. 5a). The Senonian deposits

are unconformably overlain by Miocene succession, which
416 was deposited in a prograding delta system. The related
417 clinofolds are well visible, and dip apparently towards SW
418 (Fig. 5a, b).
419

Structural geometry

The most prominent structure of the section A–A' is an
421 extensional graben, which is sealed by the Senonian deposits
422 (Fig. 5a). This graben can be traced on the northeastern part
423 of the section B–B', but it is much narrower there (Fig. 5b).
424 The graben has a segmented southwestern, NE-dipping
425 boundary fault (Fault A) and a northeastern, SW-dipping
426 boundary fault (Fault B). The graben is dissected by an addi-
427 tional NE-dipping fault (Fault C) creating two sub-grabens.
428 These faults are post-dated by Senonian; however, Fault A
429 and C show minor Senonian re-activation (Fig. 5a). On sec-
430 tion B–B', Fault C seems to be cut by a younger, probably
431 Senonian fault (Fig. 5b). The Kössen Marl forms SW-ward
432 thickening half-grabens above the gently SW-ward tilted
433 blocks, which are pronounced on section A–A' (Fig. 5a).
434 On the section B–B', the graben shows more symmetric
435 geometry (Fig. 5b). In the southwestern sub-graben, off-
436 lap surface within the Kössen Marl occurs (Fig. 5a). The
437 contact between the Dachstein Limestone and the Kössen
438 Marl is also an off-lap surface. In the vicinity of the major
439 faults, the seismic image of the Kössen Marl shows poor
440 quality, and in the hanging wall of the faults, wedge-shaped
441 bodies are outlined (Fig. 5a, b). We interpret these bodies
442 as fault-bounded talus breccia. The thickening trends of the
443 Kössen Marl suggest that Fault A and C were dominantly
444 active during its deposition (Fig. 5a, b). The Dachstein and
445 Kardosrét Limestone are gradually thickening towards Fault
446 B, which is well illustrated in section B–B' (Fig. 5b). Only
447 minor offset of these formations can be observed along the
448 other two faults (Fault A and C). Therefore, the fault activity
449 retreated onto Fault B during the deposition of the Dachstein
450 and Kardosrét Limestone. If we restore the Senonian re-
451 activation of Fault A and C, it seems that Jurassic strata
452 sealed these faults. However, Jurassic deposits occur only
453 in the hanging wall of Fault B, which suggests that the fault
454 was active during or after deposition, but before the deposi-
455 tion of Senonian rocks.
456

On the southwestern part of the section B–B', another
457 pre-orogenic graben is enclosed by Fault D and Fault E
458 (Fig. 5b). The Kössen, Dachstein, and Kardosrét Formations
459 do not have any thickness changes related to these faults. On
460 the other hand, Jurassic succession is thicker in the graben,
461 and reflections in the Jurassic seals Fault D, that suggest
462 Jurassic synsedimentary movement. Fault E is re-activated
463 by post-orogenic extension probably during Senonian and
464 Miocene; nevertheless, it shows significantly bigger pre-
465 Senonian offset (Fig. 5b).
466

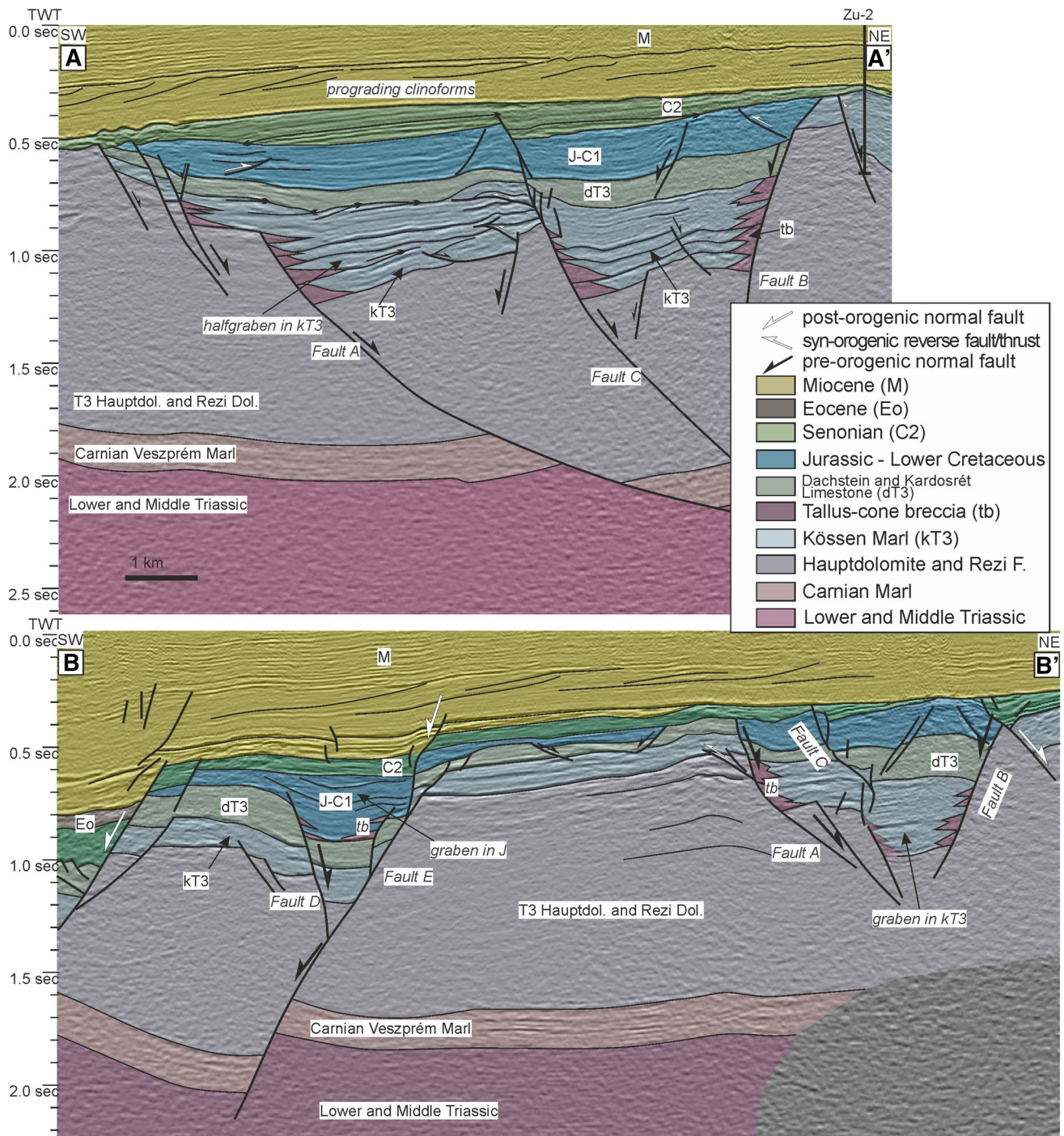


Fig. 5 a A–A' and b B–B' interpreted 2D seismic sections in the NW foreland of Keszthely Hills. Approximate location of the section is indicated in Figs. 1b and 6a. Blank version of the sections is visible in Supplementary Appendix I

467 Small normal faults are visible on the horst between
 468 Fault E and Fault A. These faults cross cut only the
 469 Dachstein and Kardosrét Limestone, and they probably
 470 detach on the Kössen Marl. These structures possibly rep-
 471 resent mega-slides (Fig. 5b).

The sections are situated in the core of the “mid”-Cre-
 taceous Sümeg-Devecser syncline (Tari 1994), and they
 are subparallel to the axis of syncline. Therefore, no major
 “mid”-Cretaceous contractional structures are visible on
 these sections. However, minor thrusts and related faults

477 occur in the pre-Senonian rocks (Fig. 5a). It is interesting
 478 that these structures are localized by the early pre-orogenic
 479 faults. In the case of Fault A and B, antithetic small thrusts
 480 developed in the proximal hanging wall of the faults within
 481 the Jurassic succession. Above/near the Fault C on top of a
 482 small horst small double verging thrusts developed in the
 483 Kössen Marl, which made a gentle anticline in the Dachstein
 484 Limestone. These compressional structures formed due to
 485 moderate Cretaceous shortening.
 486 The above-described extensional faults can be traced
 487 on other seismic sections, as well. On the bases of these
 488 2D seismic lines, the strike of these structures is between
 489 WNW–ESE and NW–SE.

490 **Interpretation of field observations**

491 **Coarse breccias along the Late Triassic**
 492 **Cserszegtomaj Fault**

493 Map-view synsedimentary normal faults can be often out-
 494 lined based on facies distribution and the presence of coarse

breccias in the proximal hanging wall of the fault (e.g., Ber-
 495 totti et al. 1993). Dolomite breccias of the Rezi Dolomite
 496 described in the outcrops of the Keszthely Hills have dolo-
 497omite matrix, which suggests that these are sedimentary breccias.
 498 These breccias re-deposited on a most probably fault-
 499controlled slope (Csillag et al. 1995). Such breccias could be
 500alternatively formed after deposition, due to seismic shock
 501of semi-unconsolidated mud (Hips et al. 2016). In the study
 502area, dolomite breccia outcrops of the Rezi Formation are
 503limited to an NW–SE-trending belt along the southwestern
 504edge of the Keszthely Hills (Fig. 6c). Coarse breccias of
 505the Csókakő quarry (L1) and the Kőmell cliff (L6) could
 506be interpreted as proximal talus breccia (Fig. 2a), while
 507the more fine-grained breccia intercalation in the Pilikán
 508quarry (L2) could be interpreted as a more distal lobe of
 509fault-related mass movements (Fig. 3b). Platform environ-
 510ment is suggested as the source of fossil-rich blocks in the
 511Csókakő quarry (L1) (Csillag et al. 1995).

512 South of the dolomite breccia occurrence of Csókakő
 513 quarry (L1) Hauptdolomit is exposed (Figs. 6a, 7a). The
 514 WNW–ESE-trending contact of the two formations was
 515 identified already by former mapping (Bohn 1979; Budai
 516

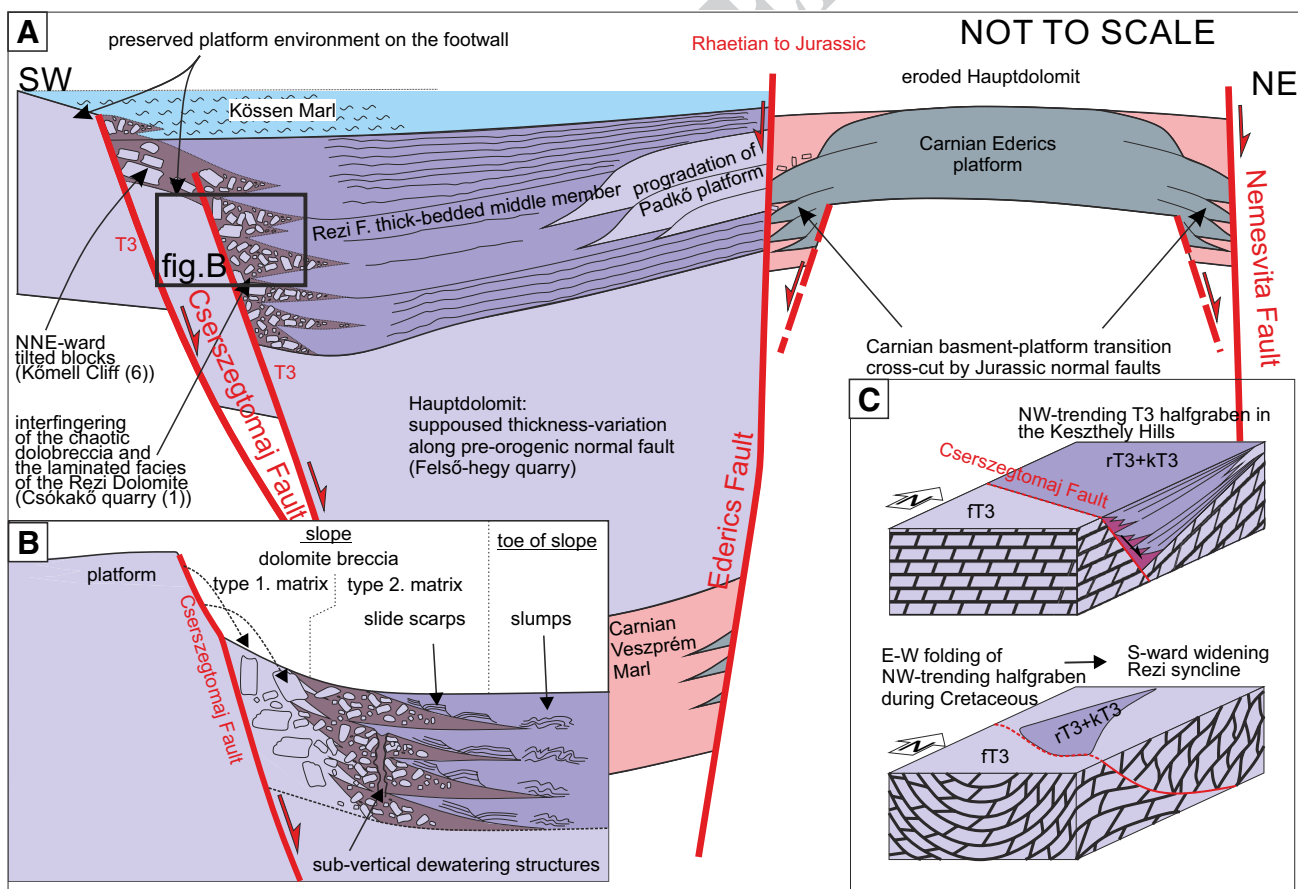


Fig. 6 a Pre-Miocene geologic map of the Keszthely Hills, and its NW foreland. b Detailed map of the Eastern Keszthely Hills. c Late Triassic synsedimentary structures along the Cserszegtomaj Fault

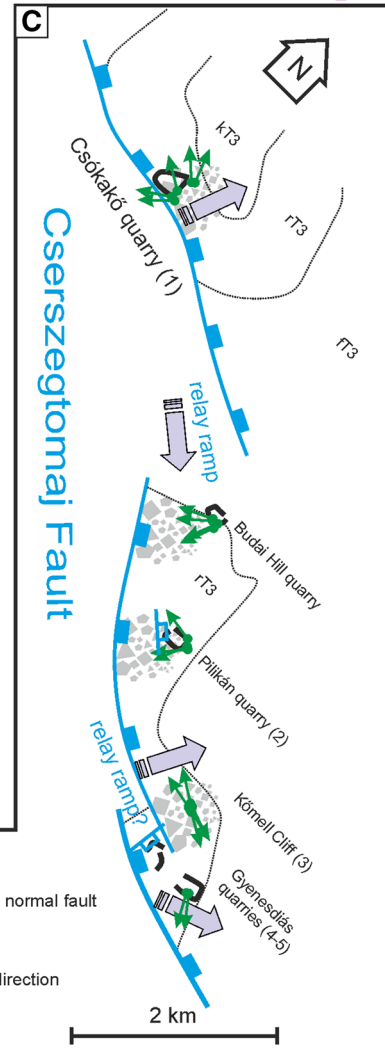
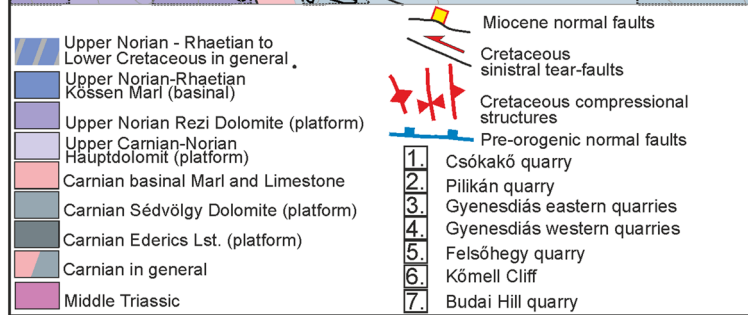
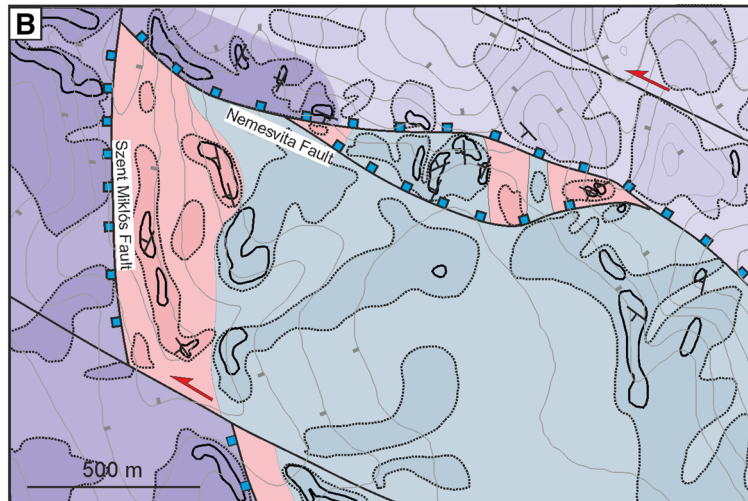
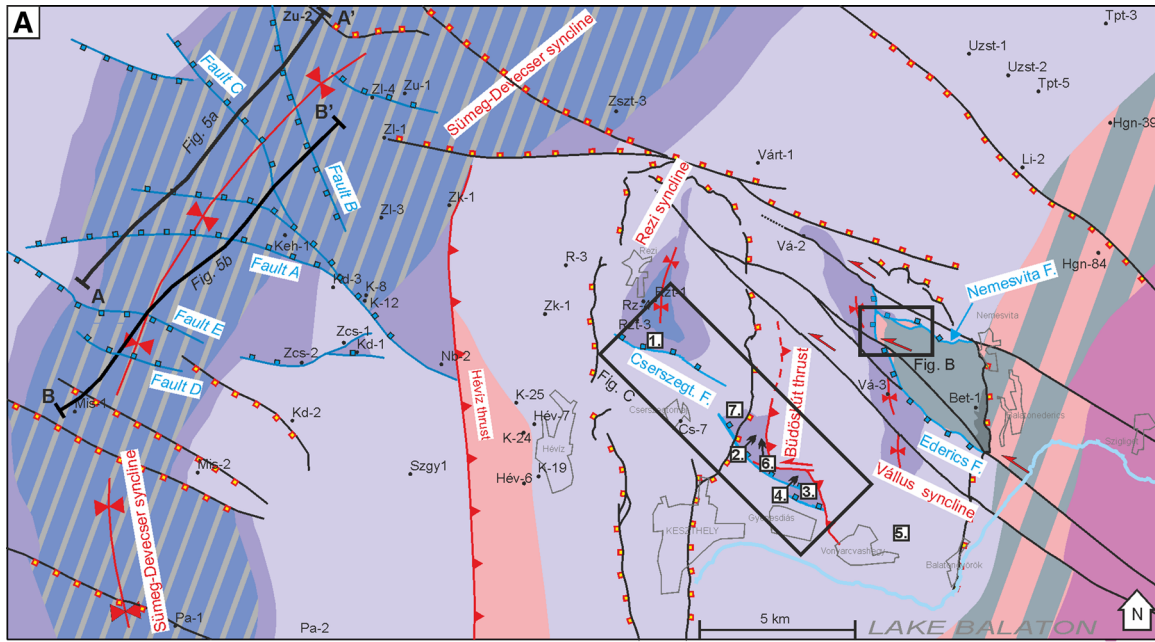


Fig. 7 **a** Model cross section across the Keszthely Hills, showing the pre-orogenic basin geometry. **b** Position of the Csókakő quarry in relationship with Cserszegtomaj fault. **c** Simplified cartoon explaining the formation of the southward widening Rezi syncline, as a folded Late Triassic half-graben

et al. 1999b); however, it was interpreted as a stratigraphic contact (Fig. 1b). In our interpretation, this contact represents a Late Triassic synsedimentary normal fault, which is referred as the Cserszegtomaj Fault in this paper (Fig. 6a). Probably, the southern WNW-trending border of the Rezi Dolomite occurrences near Gyenesdiás represents further NNE-dipping segments of Cserszegtomaj Fault, which was connected by ESE-dipping relay ramps (Fig. 6a, c).

Progradational tongue of dolomitized platform carbonates above the Rezi Dolomite was documented in the eastern part of the Keszthely Hills by Csillag et al. (1995). This pattern suggests rather asymmetric half-graben geometry for the Late Norian basin of the Keszthely Hill (Fig. 7a). Note that the southward widening geometry of the N-trending Rezi syncline could be also explained by the Cretaceous folding of a WNW–ESE-trending Late Triassic half-graben (Fig. 7c).

The Cserszegtomaj Fault can be correlated with Fault A and C introduced on seismic sections. The activity of these NE–NNE-dipping faults is evidenced by main syntectonic deposits, which is represented by Rezi Dolomite in the Keszthely Hills (Fig. 7a, b), and Kössen Marl on the seismic section (Fig. 5a, b). Probably, all of these faults were active simultaneously, although the resolution of seismic sections does not allow the observation of synsedimentary deformation of the Rezi Dolomite. The lack of Kössen Marl outcrop in the Keszthely Hills made it problematic to observe its deformation. Nevertheless, the presence of slumps and sedimentary breccias in the Kössen Marl was documented based on wells in the Keszthely Hills (Haas 1993).

547 **Rhaetian? To Jurassic extensional horst** 548 **of the eastern Keszthely Hills**

549 Reinterpretation of former geologic map (Budai et al. 1999b)
550 suggests the presence of further map-view pre-orogenic
551 structure in the Eastern Keszthely Hills. The easternmost
552 part of the Keszthely Hills (Fig. 1b) is built up by Carnian
553 formations (Csillag et al. 1995; Budai et al. 1999b). These
554 formations partly dolomitized platform carbonates (Ederics
555 Fm.) intercalating with the basinal Veszprém Marl (Csil-
556 lag et al. 1995; Budai et al. 1999b; Haas et al. 2014). The
557 Carnian formations have tectonic contact with the Rezi
558 Dolomite and the Hauptdolomit. The fault system bound-
559 ing Carnian formations has a northern WNW–ESE-trending
560 segment (Nemesvita Fault), a western N–S trending seg-
561 ment (Szent Miklós Fault), and a southern NW–SE-trending

segment (Ederics Fault) (Fig. 6a, b). The whole area is
dominated by western dips, which formed during the “mid-
Cretaceous” E–W shortening. There are areas (e.g., along
the Szent Miklós Fault), where the Carnian Veszprém Marl
is in direct contact with the Upper Norian Rezi F., and thus,
the whole Hauptdolomit, which is more than 1 km thick, is
tectonically omitted.

The Szent Miklós Fault is sub-vertical based on the vertical electric sounding of Gulyás (1991). That is why, it was interpreted by Dudko (1996) as a syn-orogenic, syn-folding strike–slip fault. In our interpretation, the large (km-scale) vertical displacement can be explained rather by normal or oblique-slip faulting (Fig. 6a, b). The actual sub-vertical dip of the fault (Gulyás 1991) can be the result of later, moderate tilting, associated with syn-orogenic Cretaceous folding, which steepened, but not overturned the original west-dipping fault.

It is clear from map view that the Szent Miklós Fault is dissected by NW–SE-trending sinistral faults with few 100 m of offset (Fig. 6a, b) (Budai et al. 1999b; Dudko 1996). These sinistral faults can be considered as syn-folding tear faults, since they have significant offset on the eastern “mid-Cretaceous” syncline (Vállus syncline); on the other hand, they die out towards northwest, and do not crosscut the western syncline (Rezi syncline). These sinistral faults were probably re-activated during the Late-Oligocene–Early Miocene, when a very similar stress field was present (Fodor et al. 1999). These sinistral faults also prove that the Szent Miklós Fault is an older, pre-orogenic fault, which was overprinted by the structures of Cretaceous compression. On the other hand, no coarse breccia was observed along the Szent Miklós Fault, which may suggest that it is younger than Rezi Dolomite.

Although there are no data on the age of Nemesvita and Ederics Fault, we suggest that these faults are coeval with the Szent Miklós Fault, and they represent a pre-orogenic extensional horst. The Ederics Fault shows many similarities to Fault B, which is slightly younger than Fault A and C. Fault B was moderately active during the deposition of Kössen Marl, but it was still active later, during the deposition of Dachstein and Kardosrét Limestone when the southwestern boundary faults (Fault A and C) were inactive (Fig. 5a). The presence of Jurassic deposits in the hanging wall and the Senonian seal suggests that Fault B was slightly active during the Jurassic, too. The same situation is suggested for the pre-orogenic horst of the eastern Keszthely Hills (Fig. 7a).

608 **Pattern of outcrop-scale pre-orogenic normal faults**

609 Many of the described faults in the Keszthely Hills can be
610 interpreted as synsedimentary Late Triassic structures, based
611 on several features. Such features are thickness variations
612 of the beds along faults (Fig. 3c, 4d, e, g), the presence of

wedge-shaped syntectonic beds (Fig. 4d, e), or faults sealed by younger beds of Late Triassic succession (Fig. 3a, c). In the Pilikán quarry (L2), small synsedimentary reverse faults occur besides normal faults. Certainly, all of these faults formed in the same extensional stress field, and the reverse faults formed due to space problems related to the movement along a non-planar normal fault plane.

Small steps of the beds in the western Gyenesdiás quarry (L4) (Fig. 4e) can be interpreted as healed normal faults, where the discrete faults disappeared due to diagenetic processes. These structures can be considered as pre-diagenetic faults. Tilted normal faults of the eastern Gyenesdiás quarry (L3) represent structures which are postdate deposition and diagenesis; on the other hand, they developed before tilting/folding, which age is Early Albian based on projection of structural data from the central Transdanubian Range (Fodor et al. 2017).

The strike of outcrop-scale synsedimentary normal faults is in accordance with map-scale pattern (Fig. 6a), since most of these structures shows NNE–SSW or NE–SW extension (Figs. 3d, 4c, h.). This direction of extension is in accordance with the trend of other pre-orogenic normal faults, described in the central and northeastern Transdanubian Range. The ages of such structures are Middle Triassic (Budai and Vörös 2006) or Early and Middle Jurassic (Vörös and Galács 1998; Lantos 1997; Fodor 2008). Perpendicular, WNW–ESE extension (Fig. 4f) was estimated based on the fault/slide of the western Gyenesdiás quarry (L4), which is situated most probably on a relay ramp which connects two segments of the Cserszegtomaj Faults (Fig. 6a).

Pattern of slumps and slides

The presence of slumps and slides is widespread in the laminated Rezi Dolomite. In the Csókakő quarry (L1), an extensional and a compressional domain can be separated, similar to many case studies (e.g., Farrell 1984; Debacker et al. 2009; Alsop and Marco 2011). We suggest that the NNE-ward-dipping beds of the southern part of the quarry represent the original dip of the slope (see next chapter). Slide scarps are present mostly in this part of the quarry (extensional domain). The northern side of the quarry, which can be characterized by horizontal dips, is dominated mostly by slumps. This part of the quarry situated on the toe of the slope where compressional domain developed.

The strike of slide scarps and slump-fold axes may allow to determine the sedimentary transport direction. The strikes of slide scarps are theoretically parallel to the strike of the slope. On the other hand, slump-fold axes can suffer notable rotation, after a significant transport (Alsop and Marco 2011). During the early stage of slump formation, the slump fold shows symmetric geometry. In that stage, the axis of the slump is perpendicular to the dip direction of the slope

(Bradley and Hanson 1998). Slumps observed in Rezi Dolomite show symmetric or slightly asymmetric geometry suggesting minor transport (e.g., Fig. 2b). Therefore, the transport direction is supposed to be sub-perpendicular to the fold axis. While most of the observed slump axes are NW–SE directed (Fig. 6c), the gravity slide transport direction is toward NE in the hanging wall of the fault segments [Csókakő quarry (L1), Kőmell Cliff (L6)] (Fig. 6c). On the other hand, the slump-fold axes pronouncedly different on relay ramps (NE-trending) which may suggest SE-ward mass transport [Budai Hill quarry (L7), Gyenesdiás quarries (L3) and (L4)] (Fig. 6c).

Slump folds often show features resembling metamorphic ductile structures; for example, the presence of stretching lineation is common in the case of soft-sediment deformation (Ortner 2013). However, in our case, a completely different type of lineation was observed. On the polished surface of samples, it is visible that this lineation derives from fold hinges of microfolds (Fig. 2b, c).

Dewatering structures

An episode of talus-cone breccia formation probably provided considerable volume of sediments. The sudden load made the underlying unconsolidated thin-layered carbonate mud compacted, and de-watered. The chaotic zone of the Csókakő quarry (L1) may indicate dewatering and fluidisation of originally laminated sediments, similar to examples of Ortner (2007). Sediment fluidization occurred where the original sedimentary features of the laminated dolomite were completely destroyed (Knipe 1986; Ortner 2007). The dewatering related compaction could be responsible for the collapse and subsidence (down bending) of overlying beds (upper laminated layer). The vertically arranged few cm zones can be interpreted as dewatering pipes, where water was released from a deeper beds (Fig. 2a). The tilted beds of the Csókakő quarry (L1) are dissected by sub-vertical dewatering pipes and fluidized zone (Figs. 2a, 7b). It confirms that the tilting in the Csókakő quarry (L1) pre-dates diagenetic processes, such as dewatering, and the tilted strata there represent the original dip of the tectonically controlled slope.

The style of the above-mentioned early deformation was probably highly influenced by the early diagenetic process such as dolomitization (Meister et al. 2013). Platform-originated re-deposited blocks observed in the Csókakő quarry (L1) (Fig. 2a) probably underwent early dolomitization, as well (Haas et al. 2012), which redound the “brittle” re-deposition, represented by blocks. On the other hand, the laminated Rezi Dolomite—which deposited in deeper marine environment—probably dolomitized later, during burial; therefore, dolomitization did not obstruct soft-sediment deformation, such as slumping or soft-sediment fluidization.

715 **Discussion: regional outlook**

716 **Comparison with other Alpine basins**

717 A newly defined Late Triassic extensional graben system
 718 was identified in this paper, which can be correlated to
 719 other areas of the Alpine region. Similar Late Triassic
 720 extensional back-platform basins are known from the west-
 721 ern Southern Alps (Lombardy) and from the Bajuvaric
 722 nappe system of the Northern Calcareous Alps. On the
 723 basis of Late Triassic facies boundaries, several authors
 724 argue that the Transdanubian Range was located more to
 725 the west, between the Northern Calcareous Alps of the
 726 Drau Range and Southern Alps (Haas et al. 1995; Mandl
 727 2000), and these Late Triassic extensional basins formed
 728 a continuous graben system, which is referred as Kössen
 729 Basin in this paper (Fig. 8a). The correlation of the related
 730 succession was the topic of several publications (Haas
 731 et al. 1995; Gale et al. 2015; Rožič et al. 2009); therefore,

in this paper, we compare these basins from a structural
 point of view.

The geometry of the Late Triassic extensional basins is well reconstructed in the Lombardy; notwithstanding, it is strongly overprinted by southvergent Cenozoic thrusts (Bertotti et al. 1993; Carminati et al. 2010; Jadoul et al. 2005). Approximately 10 km wide, N–S trending horsts and grabens were formed there, which show a similar geometry like the Late Triassic grabens of the southwestern Transdanubian Range (Bertotti et al. 1993). Bally et al. (1981) documented listric geometry for some of these faults, similar to Fault A in the present study. According to Bertotti et al. (1993), some of the Norian–Rhaetian faults in the Lombardian region were active during the Jurassic, which is also a common feature, compared to our observations. Back-rotating the units with the Mesozoic paleomagnetic data (Fig. 1a; references therein), the pre-orogenic normal faults of Lombardy and the study area have similar N–S strike (Fig. 8a).

The pre-orogenic basins in the Northern Calcareous Alps were strongly overprinted by Cretaceous and Cenozoic nappe stacking. Therefore, the Late Triassic basin

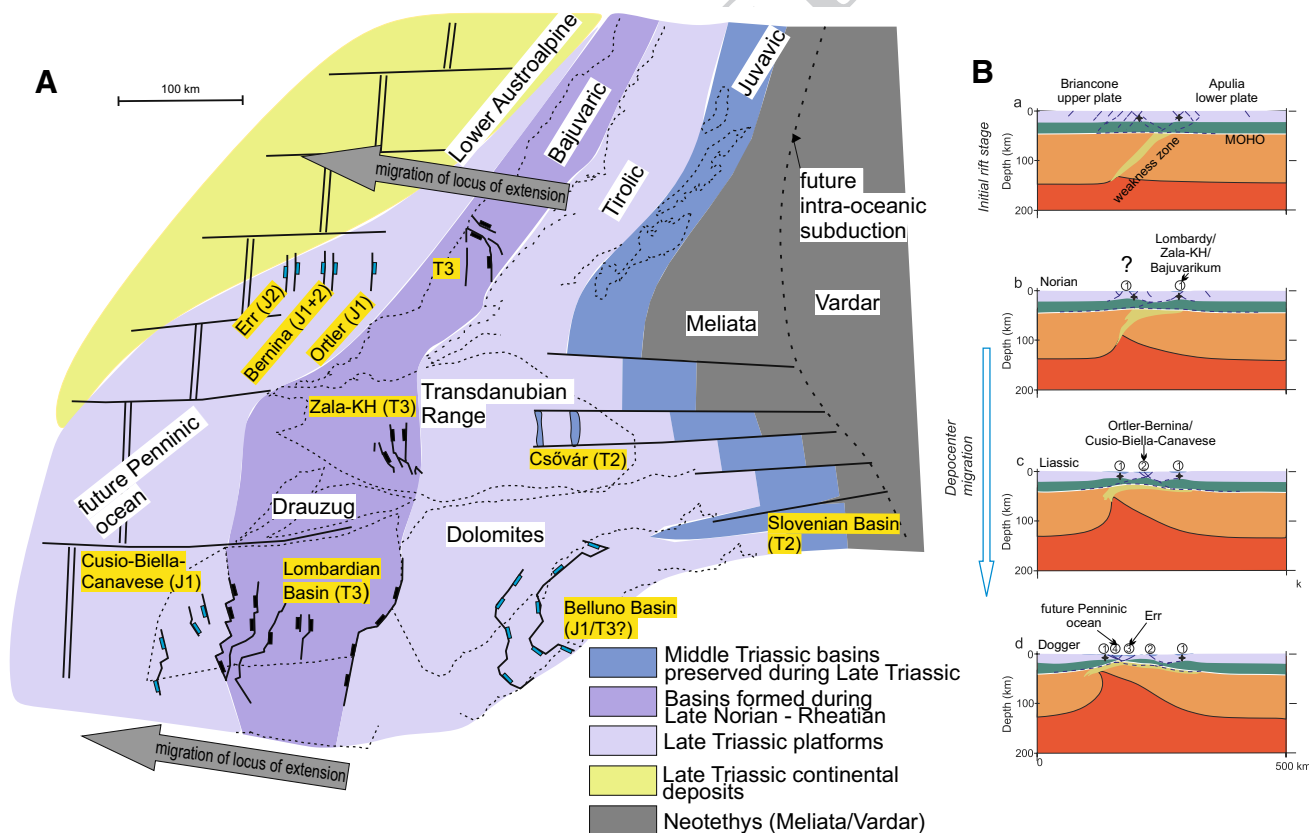


Fig. 8 a Late Triassic paleogeographic reconstruction of the Transdanubian Range and neighbour units based on Haas et al. (1995), Froitzeim and Manatschal (1996), Mandl (2000), and Gawlick et al. (1999). Fault patterns are adopted from Cazzini et al. (2015) and Behrmann and Tanner (2006). The faults were back rotated based

on the magnetization direction of Fig. 1a (see references there). **b** Migration of locus of extension on the lower Apulian plate during the opening of Piemont–Liguria ocean, applying the numerical model of Balázs et al. (2017)

753 geometry has not been reconstructed, yet from the struc-
 754 tural point of view. However, several authors propose the
 755 presence of Norian extensional deformation based on
 756 facies distribution and other sedimentological evidences
 757 (Satterley and Brandner 1995; Gawlick and Missoni 2013).
 758 An exception is the work of Behrmann and Tanner (2006),
 759 which reported the thickness variation of the Hauptdol-
 760omit along N–S and NW–SE-trending faults based on
 761 restored cross-sections. This also confirms that a signifi-
 762 cant deformation initiated already during the deposition
 763 of the Hauptdolomit. Considering paleomagnetic data
 764 (Fig. 1a; references therein), the NW–SE-trending seg-
 765ment also shows N–S paleo-trend, like in the study area
 766 (Fig. 8a).

767 Most of the Anisian basins, which were formed due
 768 to opening of the Neotethys, were filled up during the
 769 Carnian. However, in those basins, which were situated
 770 along the distal Adriatic passive margin, deep-water sedi-
 771 mentation was continuous during Late Triassic. Probably,
 772 Norian–Rhaetian extension contributed to the preserva-
 773 tion of these basins. Such basins are the Hallstatt basin of
 774 the Northern Calcareous Alps (Lein 1985; Gawlick and
 775 Böhm 2000), the Csővár and Mátyáshegy basin in the NE
 776 Transdanubian Range (Haas et al. 2010), and the Sloven-
 777 nian basin in the Southern Alps (Goričan 2012; Gale et al.
 778 2015; Celarc et al. 2013; Oprčkal et al. 2012). Accord-
 779 ing to Missoni et al. (2008), the Slovenian basin was con-
 780 trolled by strike–slip movement during Late Triassic times
 781 (Fig. 8a).

782 Geodynamic implications

783 Geodynamic background of Norian deformation of the Adri-
 784 atic plate is still under debate. Bertotti et al. (1993) con-
 785 sidered this deformation as the first sign of Alpine Tethys
 786 rifting. According to Cozzi (2000), Norian faults of the
 787 Southern Alps can be related rather to the opening of the
 788 Neotethys. Based on the recent works, continental rifting of
 789 the Alpine Tethys started just during Early Jurassic (Froitz-
 790 neim and Manatschal 1996; Berra et al. 2009; Decarlis et al.
 791 2015).

792 On the basis of the Triassic evolution of the Transdanu-
 793 bian Range, the Anisian extension, related to the opening
 794 of the Neotethys (Vörös and Budai 2006), can be clearly
 795 separated from Norian extension. Our results show that the
 796 main syn-rift sediments (Rezi and Kössen Fm.) are Late Tri-
 797 assic in age in the study area, and extension was continuous
 798 in the Jurassic. This observation may link the formation of
 799 these basins rather to the continental rifting of the Alpine
 800 Tethys. It suggests that the rifting should have started on
 801 the proximal Adriatic margin even during Norian (Bertotti
 802 et al. 1993).

Asymmetry of the Alpine Tethys rift

804 The Late Triassic Kössen basin was situated significantly to
 805 the east of the future Alpine Tethys, on the proximal Adriatic
 806 passive margin (Fig. 8a). During Jurassic, westward migra-
 807 tion of extensional tectonism was pointed out in the case of
 808 Austroalpine nappes (Froitzneim and Manatschal 1996). The
 809 proximal Adriatic margin was subject of dominantly Hettan-
 810 gian–Sinemurian extension, whereas, in the distal Adriatic
 811 margin, Pliensbachian–Callovian extension occurred (Fig. 8a).
 812 A similar situation was interpreted for the Southern Alps, west
 813 of Lombardy. In the Cusio-Biella-Canavese Zone, extensional
 814 grabens formed just during the Early Jurassic (Decarlis et al.
 815 2017).

816 Nevertheless, Jurassic normal faults and grabens are known
 817 east of the Lombardian basin. In the Belluno Basin, deep-water
 818 sedimentation and facies differentiation started just during the
 819 Early Jurassic. However, thickness changes suggest that a sig-
 820 nificant extension initiated also in the Belluno Basin during
 821 the Norian, but, in contrast with Lombardian Basin, the sedi-
 822 mentation could keep pace with extension-related subsidence
 823 (Masetti et al. 2012).

824 Most authors agree that the opening of the Piemont–Ligu-
 825 rian Ocean is the result of asymmetric rifting, where the Adri-
 826 atic plate represents the lower plate, while the European plate
 827 is the upper plate (Froitzneim and Manatschal 1996). Alterna-
 828 tively, it is also possible that the rift system changed polarity
 829 along a major transform fault, such as paleo-Periadriatic Fault
 830 (Decarlis et al. 2017). According to Lavier and Manatschal
 831 (2006) and Decarlis et al. (2017), the rift system became asym-
 832 metric only after necking of the lithosphere, when the residual
 833 crust did not contain any ductile level.

834 According to our opinion, the rifting of the Alpine Tethys
 835 was the initial asymmetric, since we connect the formation
 836 of the Late Triassic basins to the initial continental extension
 837 within the upper crust. Thus, westward migration of exten-
 838 sional deformation started during Late Triassic (Fig. 8b). This
 839 feature is asymmetric, while such processes are not present
 840 on the adjacent European margin. According to a numerical
 841 model of Balázs et al. (2017), the development of initially
 842 asymmetric rift zones can be triggered by inherited weakness
 843 zones (e.g., inherited suture). In the present case, the role of
 844 Variscan orogeny or its Permian collapse can arise (Manatschal
 845 et al. 2015). On the other hand, this relationship needs further
 846 investigation, since the built up of Variscan orogeny has been
 847 poorly reconstructed yet in the study and neighbour areas, due
 848 to strong Alpine overprint.

849 **Conclusions**

850 Late Triassic and Jurassic map-scale normal faults were
851 defined in the southeastern part of the Transdanubian Range,
852 based on field observation and 2D seismic data. The faults
853 show NW–SE-to-WNW–ESE trend. The extension was active
854 already during the deposition of the Hauptdolomit (Norian).
855 Initially, the sedimentation was able to keep pace with the
856 extension-derived subsidence, and thus, platform environment
857 was present both in the footwall and hanging wall. At the end
858 of Middle Norian, extension-related intraplatform basin of the
859 Rezi Dolomite and the Rhaetian Kössen Marl formed. The
860 extensional deformation was active during the Late Rhaetian
861 progradation of the Dachstein Limestone, and through the
862 Lower-to-Middle Jurassic. Consequently, we propose contin-
863 uous extension during the Late Triassic and Early–Middle
864 Jurassic.

865 In the Keszthely Hills, the late Middle Norian–Upper
866 Norian Rezi Dolomite is proved to be the main syntectonic
867 deposit. The synsedimentary faulting was associated with the
868 development of slides and slumps, and the formation of fault-
869 bounded talus-cone breccia.

870 Other type of pre-orogenic extensional faults post-dates
871 the deposition of Rezi Dolomite, but pre-dates Albian fold-
872 ing. These structures formed probably during the Jurassic. The
873 Szent Miklós Fault represents one map-view example of these
874 structures in the Keszthely Hills.

875 On 2D seismic section, normal faulting proved to be coeval
876 with the deposition of Kössen Marl and Dachstein Limestone.
877 The main reasons are thickness variations due to normal fault-
878 ing, and the presence of talus-cone breccia. Jurassic activity of
879 fault B was also proposed in this case.

880 The Late Triassic extension was the first sign of continental
881 rifting of Alpine Tethys, which represents an initially asym-
882 metric rift, where at least the northern part of the Adriatic
883 plate was in lower plate position. The Lombardian Basin–Zala
884 Basin–future Bajuvaric nappe system was the first locus of
885 rift-related extension on the proximal Adriatic margin. Later
886 on, during the Early and Middle Jurassic, the axis of exten-
887 sional deformation was migrated westward, towards the future
888 Alpine Tethys.

889 **Acknowledgements** This work was supported by the Hungarian
890 Researched Found OTKA 113013. Seismic data set is available by
891 MOL Hungarian Oil and Gas Plc. Quarry managers permitted the
892 access to the visited quarries (Dolomit Ltd., Molnárkő Ltd., and Pajtika
893 Ltd.). The authors are grateful to János Haas and Hugo Ortner for the
894 helpful discussion. Constructive comments of Dušan Plašienka and an
895 anonymous reviewer are appreciated.

References

- Alsop GI, Marco S (2011) Soft-sediment deformation within seismo- 897
genic slumps of the Dead Sea Basin. *J Struct Geol* 33(4):433–457. 898
<https://doi.org/10.1016/j.jsg.2011.02.003> 899
- Angelier J (1990) Inversion of field data in fault tectonics to obtain 900
the regional stress. III—A new rapid direct inversion method by 901
analytical means. *Geophys J Int* 103:363–373 902
- Balázs A, Matenco L, Magyar I, Horváth F, Cloetingh S (2016) The 903
link between tectonics and sedimentation in back-arc basins: new 904
genetic constraints from the analysis of the Pannonian Basin. 905
Tectonics 35:1526–1559. <https://doi.org/10.1002/2015TC004109> 906
- Balázs A, Burov E, Matenco L, Vogt K, François T, Cloetingh S 907
(2017) Symmetry during the syn- and post-rift evolution of 908
extensional back-arc basins: the role of inherited orogenic struc- 909
tures. *Earth Planet Sci Lett* 462:86–98. [https://doi.org/10.1016/j. 910
epsl.2017.01.015](https://doi.org/10.1016/j.epsl.2017.01.015) 911
- Balla Z (1984) The Carpathian loop and Pannonian Basin: a kinematic 912
analysis. *Geophys Trans* 30(4):313–355 913
- Bally A, Bernoulli D, Davis A, Montadert L (1981) Listric normal 914
faults. *Oceanologica Acta* 0:87–101 (**special issue (0399–1784)**) 915
- Becke M, Mauritsch HJ (1985) Die Entwicklung der Nördlichen 916
Kalkalpen ans palaomagnetischer Sicht. *Archiv für Lagerstätten- 917
forschung der Geologischen Bundesanstalt* 6:113–116 918
- Behrmann JH, Tanner DC (2006) Structural synthesis of the North- 919
ern Calcareous Alps, TRANSALP segment. *Tectonophysics* 920
414:225–240 921
- Bergerat F, Collin PY, Ganzhorn AC, Baudin F, Galbrun B, Rouget I, 922
Schnyder J (2011) Instability structures, synsedimentary faults 923
and turbidites, witnesses of a Liassic seismotectonic activity 924
in the Dauphiné Zone (French Alps): a case example in the 925
Lower Pliensbachian at Saint-Michel-en-Beaumont. *J Geodyn* 926
51(5):344–357. <https://doi.org/10.1016/j.jog.2010.10.003> 927
- Berra F, Galli MT, Reghellin F, Torricelli S, Fantoni R (2009) Strati- 928
graphic evolution of the Triassic–Jurassic succession in the West- 929
ern Southern Alps (Italy): the record of the two-stage rifting on 930
the distal passive margin of Adria. *Basin Res* 21(3):335–353 931
- Bertotti G, Picotti V, Bernoulli D, Castellarin A (1993) From rifting to 932
drifting: tectonic evolution of the South-Alpine upper crust from 933
the Triassic to the Early Cretaceous. *Sediment Geol* 86(1–2):53– 934
76. [https://doi.org/10.1016/0037-0738\(93\)90133-P](https://doi.org/10.1016/0037-0738(93)90133-P) 935
- Billi A, Salvini F (2003) Development of systematic joints in response 936
to flexure-related fibre stress in flexed foreland plates: the Apulian 937
forebulge case history, Italy. *J Geodyn* 36(4):523–536. [https://doi. 938
org/10.1016/S0264-3707\(03\)00086-3](https://doi.org/10.1016/S0264-3707(03)00086-3) 939
- Bohn P (1979) The regional geology of the Keszthely Mountains. *Geo- 940
logica Hungarica Series Geologica* 19:197 941
- Bonini M, Sani F, Antonielli B (2012) Basin inversion and contrac- 942
tional reactivation of inherited normal faults: a review based on 943
previous and new experimental models. *Tectonophysics* 522– 944
523:55–88. <https://doi.org/10.1016/j.tecto.2011.11.014> 945
- Bradley D, Hanson L (1998) Paleoslope analysis of slump folds in the 946
Devonian Flysch of Maine. *J Geol* 106(3):305–318. [https://doi. 947
org/10.1086/516024](https://doi.org/10.1086/516024) 948
- Budai T, Kolozsár L (1987) Stratigraphic investigation of the Norian- 949
Rhaetian formations in the Keszthely Mountains (in Hungarian 950
with English abstract). *Földtani Közlelöny* 117:121–130 951
- Budai T, Kovács S (1986) Contributions to the stratigraphy of the Rezi 952
Dolomite Formation [Metapolygnathus Slovagensis (conodonta, 953
Upper Triassic) from the Keszthely Mts (W Hungary)]. Annual 954
report of the Geological Institute of Hungary 1984, pp 175–191 955
- Budai T, Vörös A (2006) Middle Triassic platform and basin evo- 956
lution of the Southern Bakony Mountains (Transdanubian 957
Range, Hungary). *Rivista Italiana di Paleontologia e stratigrafia* 958
112(3):359–371 959

- 960 Budai T, Császár G, Csillag G, Dudko A, Koloszar L, Majoros G
961 (1999a) Geology of the Balaton Highland. Explanation to the
962 geological map of the Balaton Highland (1:50 000). Budapest
963 Budai T, Csillag G, Dudko A, Koloszar L (1999b) Geological map
964 of the Balaton Highland (1:50 000). Budapest
965 Butler RWH, Tavarnelli E, Grasso M (2006) Structural inheritance
966 in mountain belts: an Alpine–Apennine perspective. *J Struct*
967 *Geol* 28:1893–1908
968 Carminati E, Cavazza D, Scrocca D, Fantoni R, Scotti P, Doglioni
969 C (2010) Thermal and tectonic evolution of the southern Alps
970 (Northern Italy) rifting: Coupled organic matter maturity analy-
971 sis and thermokinematic modeling. *AAPG Bull* 94(3):369–397.
972 <https://doi.org/10.1306/08240909069>
973 Cazzini F, Zotto OD, Fantoni R, Ghielmi M, Ronchi P, Scotti P
974 (2015) Oil and gas in the adriatic foreland, Italy. *J Pet Geol*
975 38(3):255–279. <https://doi.org/10.1111/jpg.12610>
976 Celarc B, Goričan Š, Kolar-Jurkovšek T (2013) Middle Triassic
977 carbonate-platform break-up and formation of small-scale half-
978 grabens (Julian and Kamnik-Savinja Alps, Slovenia). *Facies*
979 59(3):583–610. <https://doi.org/10.1007/s10347-012-0326-0>
980 Channell JET, Brandner R, Spieler A (1990) Mesozoic paleogeog-
981 raphy of the Northern Calcareous Alps—evidence from paleo-
982 magnetism and facies analysis. *Geology* 18(9):828–831. [https://doi.org/10.1130/0091-7613\(1990\)018%3C0828:MPOTN%3E2.3.CO;2](https://doi.org/10.1130/0091-7613(1990)018%3C0828:MPOTN%3E2.3.CO;2)
983
984 Cozzi A (2000) Synsedimentary tensional features in Upper Triassic
985 shallow-water platform carbonates of the Carnian Prealps (north-
986 ern Italy) and their importance as palaeostress indicators. *Basin*
987 *Res* 12:133–146
988 Császár G, Gyalog L (1982) Pre-Quaternary geological map of the
989 Bakony Mountains (1:50 000). Budapest
990 Csillag G, Budai T, Gyalog L, Koloszar L (1995) Contribution to the
991 Upper Triassic geology of the Keszthely Mountains (Transdanu-
992 bian Range), western Hungary. *Acta Geol Hung* 38(2):111–129
993 Csontos L, Nagymarosy A (1998) The Mid-Hungarian line: a zone of
994 repeated tectonic inversions. *Tectonophysics* 297:51–71. [https://doi.org/10.1016/S0040-1951\(98\)00163-2](https://doi.org/10.1016/S0040-1951(98)00163-2)
995
996 Csontos L, Vörös A (2004) Mesozoic plate tectonic reconstruction of
997 the Carpathian region. *Palaeogeogr Palaeoclimatol Palaeoecol*
998 210(1):1–56. <https://doi.org/10.1016/j.palaeo.2004.02.033>
999
1000 De Vicente G, Vegas R, Muñoz-Martín A, Van Wees JD, Casas-
1001 Sáinz A, Sopena A, Fernández-Lozano J (2009) Oblique strain
1002 partitioning and transpression on an inverted rift: the Castilian
1003 Branch of the Iberian Chain. *Tectonophysics* 470(3–4):224–242.
1004 <https://doi.org/10.1016/j.tecto.2008.11.003>
1005 Debacker TN, Dumon M, Matthys A (2009) Interpreting fold
1006 and fault geometries from within the lateral to oblique parts
1007 of slumps: a case study from the Anglo-Brabant Deformation
1008 Belt (Belgium). *J Struct Geol* 31:1525–1539. <https://doi.org/10.1016/j.jsg.2009.09.002>
1009
1010 Decarlis A, Manatschal G, Hauptert I, Masini E (2015) The tectono-
1011 stratigraphic evolution of distal, hyper-extended magma-poor
1012 conjugate rifted margins: examples from the Alpine Tethys and
1013 Newfoundland Iberia. *Mar Pet Geol* 68:54–72
1014 Decarlis A, Beltrando M, Manatschal G, Ferrando S, Carosi R (2017)
1015 Architecture of the distal Piedmont-Ligurian rifted margin in
1016 NW Italy: hints for a flip of the rift system polarity. *Tectonics*
1017 36(11):2388–2406. <https://doi.org/10.1002/2017TC004561>
1018 Dohr G (1981) Geophysikalische Untersuchungen im Gebiet der
1019 Tiefbohrung Vorderriß 1. *Geologica Bavarica* 81:55–64 (**6**
1020 **Abb., München**)
1021 Dudko A (1996) A Balaton-felvidék szerkezete (fedetlen földtani
1022 térkép alapján) (Translated title: structure of the Balaton High-
1023 land (based on pre-Quaternary geological map)). manuscript.
1024 Geological Institute of Hungary, Budapest
- Farrell SG (1984) A dislocation model applied to slump structures,
Ainsa Basin, South Central Pyrenees. *J Struct Geol* 6:727–736 1025
Fodor L (2008) Structural geology. In: Budai T, Fodor L (eds) Explana- 1026
tory book to the geological map of the Vértes Hills (1:50 000). 1027
Budapest, pp 282–302 1028
Fodor L, Csontos L, Bada G, Györfi I, Benkovic L (1999) Tertiary 1029
tectonic evolution of the Pannonian basin system and neighbour- 1030
ing orogens: a new synthesis of paleostress data. In: Durand B, 1031
Jolivet L, Horváth F, Séranne M (eds) *The Mediterranean basins: 1032*
tertiary extension within the Alpine Orogen, vol 156. Geological 1033
Society, Special Publications, London, pp 295–334 1034
Fodor L, Uhrin A, Palotás K, Selmecei I, Tóthné Makk Á, Rižnar I, 1035
Trajanova M, Rifelj H, Jelen B, Budai T, Koroknai B, Mozetič S, 1036
Nádor A, Lapanje A (2013) Geological and structural model of 1037
the Mura–Zala Basin and its rims as a basis for hydrogeological 1038
analysis (in Hungarian with English abstract). Annual report of 1039
the Geological Institute of Hungary 2011, pp 47–92 1040
Fodor L, Héja G, Kövér Sz, Csillag G, Csicsék AL (2017) Cretaceous 1041
deformation of the south-eastern Transdanubian Range Unit, and 1042
the effect of inherited Triassic–Jurassic normal faults. Pre-con- 1043
ference excursion guide, 15th meeting of the Central European 1044
Tectonic Studies Group (CETeG) 5–8th April 2017 Zánka, Lake 1045
Balaton. *Acta Mineralogica-Petrographica, Field Guide Series* 1046
32, pp 47–76 1047
Froitzneim N, Manatschal G (1996) Kinematics of Jurassic rifting, 1048
mantle exhumation, and passive-margin formation in the Aus- 1049
troalpine and Penninic nappes (eastern Switzerland). *Bull Geol* 1050
Soc Am 108(9):1120–1133. [https://doi.org/10.1130/0016-7606\(1996\)108%3C1120:KOJRM%3E2.3.CO;2](https://doi.org/10.1130/0016-7606(1996)108%3C1120:KOJRM%3E2.3.CO;2) 1051
Fruth I, Scherrek R (1984) Hauptdolomit—sedimentary and paleo- 1052
geographic models (Norian, Northern Calcareous Alps). *Geol* 1053
Rundsch 73(1):305–319 1054
Gale L, Celarc B, Caggiati M, Kolar-Jurkovsek T, Jurkovsek B, Gia- 1055
nolla P (2015) Paleogeographic significance of Upper Triassic 1056
basinal succession of the Tamar Valley, northern Julian Alps 1057
(Slovenia). *Geol Carpath* 66(4):269–283. <https://doi.org/10.1515/geoca-2015-0025> 1058
Gallet Y, Krystyn L, Besse J (1998) Upper Anisian to Lower Carnian 1059
magnetostratigraphy from the Northern Calcareous Alps (Austria). 1060
J Geophys Res 103(B1):605–621 1061
Gawlick HJ, Böhm F (2000) Sequence and isotope stratigraphy of Late 1062
Triassic distal periplatform limestones from the Northern Calcareous 1063
Alps (Kälberstein Quarry, Berchtesgaden Hallstatt Zone). *Int* 1064
J Earth Sci 89:108–129 1065
Gawlick HJ, Missoni S (2013) Triassic to Early Cretaceous geodynamic 1066
history of the central Northern Calcareous Alps (Northwestern 1067
Tethyan realm). *Berichte Geol B A* 99:178–190 1068
Gawlick HJ, Frisch W, Vecsei A, Steiger T, Böhm F (1999) The 1069
change from rifting to thrusting in the Northern Calcareous Alps 1070
as recorded in Jurassic sediments. *Geol Rundsch* 87(4):644–657. 1071
<https://doi.org/10.1007/s005310050237> 1072
Goričan S (2012) Mesozoic deep-water basins of the eastern Southern 1073
Alps (NW Slovenia). *IAS Field Trip Guidebook*, pp 101–143 1074
Gulyás Á (1991) Jelentés a Keszthelyi-hegység és a Bakonyban 1075
1990-ben a Plató program keretében végzett felszíni geofizikai 1076
mérésekről. (translated title: report of near-surface geophysical 1077
measurement of Keszthely Hills and Bakony, Plató project 1990) 1078
manuscript, Budapest 1079
Haas J (1993) Formation and evolution of the “Kösseni Basin” in the 1080
Transdanubian Range. *Földtani Közlöny* 123(1):9–54 1081
Haas J (2002) Origin and evolution of late triassic backplatform and 1082
intraplatform basins in the Transdanubian Range, Hungary. *Geol* 1083
Carpath 53(3):159–178 1084
Haas J, Jocháné-Edelényi E, Gidai L, Kaiser M, Kretzoi M, Oravec J 1085
(1984) Geology of the Sümeg Area. *Geologica Hungarica Series* 1086
Geologica 20:353 1087
1088
1089
1090

- 1091 Haas J, Kovács S, Krystyn L, Lein R (1995) Significance of Late
1092 Permian-Triassic facies zones in terrane reconstructions in the
1093 Alpine-North Pannonian domain. *Tectonophysics* 242(1–2):19–
1094 40. [https://doi.org/10.1016/0040-1951\(94\)00157-5](https://doi.org/10.1016/0040-1951(94)00157-5)
- 1095 Haas J, Götz AE, Pálffy J (2010) Late Triassic to early Jurassic palaeo-
1096 geography and eustatic history in the NW Tethyan realm: new
1097 insights from sedimentary and organic facies of the Csővár Basin
1098 (Hungary). *Palaeogeography, Palaeoclimatology, Palaeoecology*
1099 291(3–4):456–468. <https://doi.org/10.1016/j.palaeo.2010.03.014>
- 1100 Haas J, Budai T, Raucsik B (2012) Climatic controls on sedimentary
1101 environments in the Triassic of the Transdanubian range (Western
1102 Hungary). *Palaeogeography, palaeoclimatology, Palaeoecology*
1103 353–355:31–44. <https://doi.org/10.1016/j.palaeo.2012.06.031>
- 1104 Haas J, Budai T, Györi O, Kele S (2014) Multiphase partial and selec-
1105 tive dolomitization of Carnian reef limestone (Transdanubian
1106 Range, Hungary). *Sedimentology* 61(3):836–859. <https://doi.org/10.1111/sed.12088>
- 1107 Heer L (1982) Paläomagnetische Testuntersuchungen in den Nördli-
1108 chen Kalkalpen im Gebiet zwischen Golling und Kössen. M.Sc.
1109 Thesis, Technical University, Munich
- 1110 Hips K, Haas J, Györi O (2016) Hydrothermal dolomitization of basinal
1111 deposits controlled by a synsedimentary fault system in Trias-
1112 sic extensional setting, Hungary. *Int J Earth Sci (Geol Rundsch)*
1113 105:1215–1231. <https://doi.org/10.1007/s00531-015-1237-4>
- 1114 Horváth F, Musitz B, Balázs A, Végh A, Uhrin A, Nádor A, Wórum
1115 G (2015) Evolution of the Pannonian basin and its geothermal
1116 resources. *Geothermics* 53:328–352. <https://doi.org/10.1016/j.geothermics.2014.07.009>
- 1117
1118
1119 Jadoul F, Galli MT, Calabrese L, Gnaccolini M (2005) Stratigraphy of
1120 Rhaetian To Lower Sinemurian Carbonate Platforms in Western
1121 Lombardy (Southern Alps, Italy): paleogeographic implications.
1122 *Rivista Italiana Di Paleontologia E Stratigrafia* 111(2):285–303
- 1123 Knipe RJ (1986) Deformation mechanism path diagrams for sediments
1124 undergoing lithification. *Mem Geol Soc Am* 166:151–160
- 1125 Kőrössi L (1988) Hydrocarbon geology of the Zala Basin in Hungary
1126 (in Hungarian). *Általános Földtani Szemle* 23:3–162
- 1127 Lantos Z (1997) Sediments of a Liassic carbonate slope controlled
1128 by strike-slip fault activity (Gerecse Hills, Hungary). *Földtani*
1129 *Közlöny* 127(3–4):291–320
- 1130 Lavier L, Manatschal G (2006) A mechanism to thin the continental
1131 lithosphere at magma-poor margins. *Nature* 440:324–328
- 1132 Lein R (1985) Das Mesozoikum der Nördlichen Kalkalpen als Beispiel
1133 eines gerichteten Sedimentationsverlaufes infolge fortschreitender
1134 Krustenausdünnung. *Arch F Lagerstförsch Geol B A* 6:117–128
- 1135 Manatschal G, Lavier L, Chenin P (2015) The role of inheritance
1136 in structuring hyperextended rift systems: some considerations
1137 based on observations and numerical modeling. *Gondwana Res*
1138 27:140–164
- 1139 Mandl GW (2000) The Alpine sector of the Tethyan shelf—examples
1140 of Triassic to Jurassic sedimentation and deformation from the
1141 Northern Calcareous Alps. *Mitt Österr Geol Ges* 92:61–77
- 1142 Márton E, Márton P (1983) A refined polar wander curve for the Trans-
1143 danubian Central Mountains and its bearing on the Mediterranean
1144 tectonic history. *Tectonophysics* 98:43–57
- 1145 Masetti D, Fantoni R, Romano R, Sartorio D, Trevisani E (2012)
1146 Tectonostratigraphic evolution of the Jurassic extensional basins
1147 of the eastern southern Alps and Adriatic foreland based on an
1148 integrated study of surface and subsurface data. *AAPG Bull*
1149 96(11):2065–2089. <https://doi.org/10.1306/03091211087>
- 1150 Mauritsch HJ (1980) Palaomagnetische Untersuchungen an einigen
1151 Magnesiten aus der westlichen Grauwackenzone. *Mitt Österr Geol*
1152 *Ges* 73:1–4
- 1153 Mauritsch HJ, Becke M (1987) Palaeomagnetic Investigations in the
1154 Eastern Alps and the Southern Border Zone. In: Flugel HW, Faupl
P (eds) *Geodynamics of the Eastern Alps*. Deuticke, Vienna, pp 283–308
- Mauritsch HJ, Frisch W (1978) Palaeomagnetic data from the Cen-
tral part of the Northern Calcareous Alps, Austria. *J Geophys*
44:623–637
- Meister P, McKenzie JA, Bernasconi SM, Brack P (2013) Dolomite
formation in the shallow seas of the Alpine Triassic. *Sedimentol-
ogy* 60(1):270–291. <https://doi.org/10.1111/sed.12001>
- Missoni S, Gawlick HJ, Dumitrică P, Krystyn L, Lein R (2008) Late
Triassic mass-flow deposits in hemipelagic “Slovenian Trough”-
like sediments in the Karavank Mountains (Austria) triggered by
Late Triassic strike-slip movements. *J Alp Geol* 49:71
- Oprčkal P, Gale L, Kolar-Jurkovič T, Rožič B (2012) Outcrop-scale
evidence for the Norian-Rhaetian extensional tectonics in the
Slovenian Basin (Southern Alps) (in Slovenian with English
abstract). *Geologija* 55(1):45–56. <https://doi.org/10.5474/geologija.2012.003>
- Ortner H (2007) Styles of soft-sediment deformation on top of a
growing fold system in the Gosau Group at Muttekopf, Northern
Calcareous Alps, Austria: slumping versus tectonic deformation. *Sediment Geol* 196(1–4):99–118. <https://doi.org/10.1016/j.sedgeo.2006.05.028>
- Ortner H (2013) Deep water sedimentation on top of a growing oro-
genic wedge—interaction of thrusting, erosion and deposition in
the Cretaceous Northern Calcareous Alps. *GeoAlp* 13:141–182
- Ortner H, Ustaszewski M, Rittner M (2008) Late Jurassic tectonics and
sedimentation: Breccias in the Unken syncline, central Northern
Calcareous Alps. *Swiss J Geosci*. <https://doi.org/10.1007/s00015-008-1282-0>
- Pace P, Di Domenica A, Calamita F (2014) Summit low-angle faults in
the Central Apennines of Italy: younger-on-older thrusts or rotated
normal faults? Constraints for defining the tectonic style of thrust
belts. *Tectonics* 33(5):756–785. <https://doi.org/10.1002/2013TC003385>
- Perez ND, Horton BK, Carlotto V (2016) Structural inheritance and
selective reactivation in the central Andes: Cenozoic deformation
guided by pre-Andean structures in southern Peru. *Tectonophysics*
671:264–280. <https://doi.org/10.1016/j.tecto.2015.12.031>
- Rožič B, Kolar-Jurkovič T, Šmuc A (2009) Late Triassic sedimentary
evolution of Slovenian Basin (eastern Southern Alps): description
and correlation of the Slatnik Formation. *Facies* 55(1):137–155.
<https://doi.org/10.1007/s10347-008-0164-2>
- Satterley AK, Brandner R (1995) The genesis of Lofer cycles of the
Dachstein Limestone, Northern Calcareous Alps, Austria. *Geol*
Rundsch 84(2):287–292. <https://doi.org/10.1007/BF00260441>
- Schmid SM, Bernoulli D, Fügenschuh B, Matenco L, Schefer S, Schuster R, Tischler M, Ustaszewski K (2008) The Alpine-Carpathian-Dinaridic orogenic system: correlation and evolution of tectonic units. *Swiss J Geosci* 101:139–183. <https://doi.org/10.1007/s00015-008-1247-3>
- Tari G (1994) Alpine tectonics of the Pannonian Basin. Ph.D. dissertation Rice University, Houston
- Ustaszewski K, Schmid SM (2006) Control of preexisting faults on geometry and kinematics in the northernmost part of the Jura fold-and-thrust belt. *Tectonics* 25(5):26. <https://doi.org/10.1029/2005TC001915>
- Vörös A, Galács A (1998) Jurassic palaeogeography of the Transdanubian Central Range (Hungary). *Rivista Italiana Di Paleontologia E Stratigrafia* 104(1):69–84
- Yagupsky DL, Cristallini EO, Fantín J, Valcarce GZ, Bottesi G, Varadé R (2008) Oblique half-graben inversion of the Mesozoic Neuquén Rift in the Malargüe Fold and Thrust Belt, Mendoza, Argentina: new insights from analogue models. *J Struct Geol* 30(7):839–853. <https://doi.org/10.1016/j.jsg.2008.03.007>

Author Query Form

Please ensure you fill out your response to the queries raised below and return this form along with your corrections

Dear Author

During the process of typesetting your article, the following queries have arisen. Please check your typeset proof carefully against the queries listed below and mark the necessary changes either directly on the proof/online grid or in the 'Author's response' area provided below

Query	Details Required	Author's Response
AQ1	Author: Kindly check and confirm the city and country in affiliations.	
AQ2	Author: Ref. Bergerat et al. 2010 has been changed as Bergerat et al. 2011, so that it matches the list.	
AQ3	Author: Reference: References (Goričan et al. 2012, Vörös and Budai 2006) was mentioned in the manuscript; however, this was not included in the reference list. As a rule, all mentioned references should be present in the reference list. Please provide the reference details to be inserted in the reference list.	
AQ4	Author: Please revise the sentence "From the Barremian ..." for clarity, since the sentence seems to be unclear.	
AQ5	Author: Appendix I has been changed as Supplementary Appendix I, kindly check and confirm.	
AQ6	Author: Kindly check authors initials and also provide publisher location for Ref. Fodor (2008).	